STRUCTURAL CONTROL AND HEALTH MONITORING
*Struct. Control Health Monit.* 2008; **15**:471–504
Published online 15 May 2007 in Wiley InterScience
(www.interscience.wiley.com) DOI: 10.1002/stc.205

# An experimental investigation of the data delivery performance of a wireless sensing unit designed for structural health monitoring

Jin-Song Pei[1,*,†,‡], Chetan Kapoor[2,§], Troy L. Graves-Abe[3,§], Yohanes P. Sugeng[1,¶] and Jerome P. Lynch[4,‡]

[1] *School of Civil Engineering and Environmental Science, University of Oklahoma, Norman, OK 73019-1024, U.S.A.*
[2] *School of Electrical and Computer Engineering, University of Oklahoma, Norman, OK 73019-1024, U.S.A.*
[3] *Department of Electrical Engineering, Princeton University, Princeton, NJ 08544, U.S.A.*
[4] *Department of Civil and Environmental Engineering, University of Michigan, Ann Arbor, MI 48109, U.S.A.*

## SUMMARY

This study explores the reliability of a wireless sensing unit by testing it in a real-world university laboratory environment. The unit employs off-the-shelf products for their key components, while a flexible payload scheme was adopted for radio packet transmission to maximize throughput and minimize latency. The testing consists of two main parts: (1) a series of loopback tests using two off-the-shelf radio components with carrier frequencies of 900 MHz and 2.4 GHz, respectively, and (2) wireless transmission of a shake table response to a periodic swept sine excitation. The performance of the wireless channel is examined in each part of the study. Through this experimental investigation, it is validated that a loopback test may be used as a fast prototyping approach to characterize the complex transmitting environment of a structure in which a wireless monitoring system is installed. Various factors leading to signal attenuation are ranked according to their effects on packet delivery performance. Transmitting range and building materials are among the leading factors causing packet loss (and therefore data loss) in this specific testing environment. The severity of interference from 802.11b wireless systems in close proximity to the wireless sensing unit was investigated. Some preliminary results on the influence of operating rotating machinery and human activities are to wireless sensors were investigated. The results presented herein offer a guideline for applying wireless sensing within real-world structures so that the reliability of the wireless monitoring system is maximized. Due to uncertainties associated with the reliability of wireless communications, statistical analysis is performed on the collected time histories to reveal the underlying patterns associated with data loss. Temporal correlations of data loss were measured and found to be related to the adopted radio. A statistical distribution of the size of consecutive lost data points was further derived from the collected data. Such results have identified the need to further develop: (1) reliable communication

*Correspondence to: Jin-Song Pei, School of Civil Engineering and Environmental Science, University of Oklahoma, Norman, OK 73019-1024, U.S.A.
[†]E-mail: jspei@ou.edu
[‡]Assistant Professor.
[§]Former Graduate Student.
[¶]Graduate Student.

Contract/grant sponsor: National Science Foundation; contract/grant number: SGER CMS-0332350

*Received 5 March 2006*
*Revised 28 January 2007*
*Accepted 29 January 2007*

protocols to reduce these losses in data and information, and (2) robust data processing and system identification tools to anticipate and explicitly handle any data loss. Copyright © 2007 John Wiley & Sons, Ltd.

KEY WORDS: structural health monitoring; wireless sensing; data delivery performance

## 1. INTRODUCTION

This paper is aimed at understanding how the reliability of a wireless communication channel of a wireless sensing unit will impact data processing and system identification for structural health monitoring. Wireless units were developed mostly by utilizing commercial off-the-shelf components, and a series of experiments were carried out to systematically identify the real-world challenges caused by packet and data losses. In general, the reliability of the wireless communication channel can be reduced by noise, path losses, multi-path effects, and physical interference, which can all lead to delayed transmission of data, loss of transmitted packets, and consequently, the loss of transmitted data. This is a practical issue that has been recognized as a critical technical limitation of wireless communications that must be addressed to assure the performance and reliability of wireless technology [1]. After years of active research, there exists a large body of literature dedicated to understanding this issue, for example, Seidel and Rappaport [2], Wang and Moayeri [3], Lee and Chanson [4], Tang and McKinley [5], Zhao and Govindan [6], all report on the investigation of the propagation of wireless signals. In addition, technical solutions, such as frequency hopping spread spectrum techniques [7, 8], reliable upper network protocol layers, i.e. TCP/IP communication protocols [9], are all solutions offered to address the possible loss of wireless signals.

In structural health monitoring and control, some literature has recently emerged that focuses on the fertile cross-disciplinary research area of wireless monitoring systems [10–15]. It has been less than a decade since this technology was specifically introduced to the community [16]. Successes have been achieved in the development of academic wireless sensing unit prototypes to which arbitrary analog sensors can be interfaced [17, 18], wireless data transmission in decentralized sensor network architectures, and embedded processing performed using digital signal processing cores [19]. In addition to these efforts, stand-alone wireless sensors and sensor networks have also been explored by the civil engineering community for monitoring applications [20–22]. With respect to the reliability of wireless sensing, a noticeable loss of packets using Crossbow MICA wireless when operated in streaming mode was first cited in Casciati *et al*. [23]. Data loss during the testing of the same wireless sensor platform (Crossbow MICA Mote) was reported in another study [20]. To highlight the importance of this reliability issue, Seth *et al*. [24] pointed out that latency and data loss can greatly impair the performance of a closed-loop control system implemented on a wireless sensor network. In structural health monitoring, there are still many critical issues that have yet to be fully explored regarding the reliability of wireless sensing. For example, the severity of data loss, the patterns associated with data loss, the impact such losses have on data processing and system identification, and remedies that address the issue in terms of cost and benefit all need to be explored.



DOI: 10.1002/stc

To identify these aforementioned challenges and to provide a foundation for further investigation, the authors carry out this investigation to build a wireless data channel, transmit real vibration data in a real-world environment, collect data in a *near real-time* fashion, and quantitatively study data delivery performance. It is important to highlight that the focus of this study is given to near real-time data collection, which is always desired by structural health monitoring systems to assist timely decision making under extreme events (e.g. earthquakes). Such a focus makes the reliability issue more prominent because truly real-time or even near real-time monitoring would give little or no time for 're-try' or 're-send' options when data are lost by the wireless communication system. This again justifies the significance of this study. The objectives of this experimental study can be outlined as follows:

1. Develop a wireless sensing unit that enables a systematic investigation of issues related to the reliability of the wireless communication channel. Design constraints include: (1) the use of off-the-shelf components as often as possible; (2) the need for the unit to be adaptable to various combinations of hardware options, such as the inclusion of analog-to-digital converters (ADCs) with different resolutions and radios operating on different frequencies; and (3) the employment of a data collection mechanism that is able to precisely reflect any data loss.
2. Test the performance of the developed unit in a real-world situation to reveal the influence various environmental factors have on the attenuation of wireless signals including the transmitting range through various building materials (e.g. steel walls and roofs). The tests performed herein rank the influence that these factors have on the quality of wireless communication, if possible.
3. Validate the appropriateness of loopback tests as a proper means to rapidly characterize a transmitting environment for applications in structural health monitoring. Loopback tests are important to allow for a quick and low-cost assessment of the electromagnetic (EM) environment in which a structure owner/manager will install a wireless monitoring system.
4. Investigate data delivery performance and features of data loss to aid further efforts in data processing, system identification, and the development of more robust communication protocols.

Figure 1 provides the scope of this study by outlining the broader context in which this work fits. Specifically, the study's significance is highlighted and future research directions are identified.

## 2. TESTING ENVIRONMENT AND TECHNICAL CHALLENGES

### *2.1. Overview of reliability of wireless communication*

A major factor impairing the performance of a wireless system is signal attenuation, a phenomenon that is caused by (1) beam divergence as the signal spreads while travelling away from its source (e.g. an antenna), and (2) the absorption of signal EM energy by the propagation medium. In regard to terminology, *path loss* refers to the loss of energy, while *packet loss* refers to the loss of packets; a *packet* refers to the smallest unit of information transmitted by a radio. In wireless communication, data are sent through packets with one packet containing one or multiple data points (DPs), or even partial DPs, depending on how the packets are designed [9];



DOI: 10.1002/stc

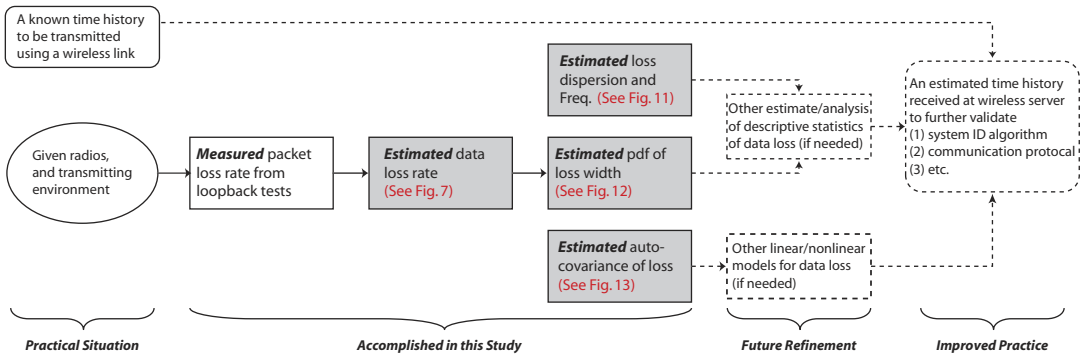


Figure 1. Scope of this study and the broad overview of the major challenges associated with wireless structural monitoring.

therefore, packet loss ultimately leads to data loss. Even though packet loss and data loss are inherently related, the feature of packet loss may or may not be equivalent to those of data loss. In the application of structural health monitoring, *data loss* is clearly the primary concern rather than packet or path loss since the processing tasks of the monitoring system are data centric. On the basis of this realization, this study is dedicated to identifying data loss issues in a wireless monitoring system so as to directly benefit the community of structural health monitoring.

For an ideal condition where there is a direct visible path between the transmitter and the receiver, i.e. line of sight (LOS), and the signal absorption is moderate to insignificant, the power received at a particular point away from the transmitter is primarily determined by beam divergence, following an inverse-square dependence on distance as given by the following equation (e.g. [7]):

$$P_r(d) = \frac{P_t G_r G_t \lambda^2}{(4\pi)^2 d^2 L} \tag{1}$$

This equation indicates the roles played by the transmitting power of the radio ($P_t$), transmitting antenna ($G_t$) and receiving antenna ($G_r$), carrier wavelength ($\lambda$), and transmitting range ($d$). Due to the presence of man-made obstacles (buildings and other structures) and natural obstructions (mountains, trees, etc.), the path between the transmitter and the receiver is often indirect (i.e. not LOS). The radio signal reaches the receiver through the processes of reflection, diffraction, and scattering and requires more complicated (and often empirical) modelling instead of using the generic loss factor of $L$ in the above equation.

Many different propagation models are available that provide estimates for the effects of signal distortion and *path loss*. Most often, these models combine empirical measurements with physics-based propagation models to account for the different ways in which a radio signal travels. Examples include the Okumura–Hata propagation model as often cited in standard communication texts (e.g. [7, 8]), and another model in Har *et al.* [25] based on a study conducted in San Francisco and Manhattan by considering the orientation of the streets, the heights of buildings within the communication range, and the heights of the transmitter and receiver as chief parameters that influence path loss. Seidel and Rappaport [2] presented equal path loss contour plots for office buildings based on experimental results at 914 MHz. A mean



DOI: 10.1002/stc

path loss was predicted to exponentially increase with the transmitting range, while the effects of walls, floors and partitions were considered using various attenuation factors.

In terms of *packet loss*, there is a vast body of knowledge on the reliability of wireless communications. Packet delivery performance has been simulated based on various models. For example, Wang and Moayeri [3] used finite-state Markov chains to model a specific wireless channel, while Lee and Chanson [4] offered a closed-form solution for packet loss probability. Altman *et al*. [26] modelled packet loss in a TCP/IP environment, while Tang and McKinley [5] simulated packet loss in a wireless local area network. For off-the-shelf wireless sensor networks, Zhao and Govindan [6] studied packet delivery performance of a Crossbow MICA sensor network with 40–60 nodes in three different testing environments, thereby providing a measure of the spatial correlation of packet losses.

Despite all these previous studies, there remains a gap between state of practice of installing wireless sensors in a civil structure and subsequent data processing (e.g. system identification). This is what will be addressed in this study, namely a systematic investigation of *data loss*.

### *2.2. Transmitting environment*

All of the experiments reported in this study were performed inside and/or in the vicinity of the Fears Structural Engineering Laboratory (abbreviated as Fears Lab hereafter) at the University of Oklahoma. The laboratory is located in an open terrain landscape on the south campus of the university where the buildings are low-rise and sparse as shown in Figure 2(a). The surrounding areas have a slightly higher elevation than the laboratory. Around some of the buildings in the testing area there are a number of large trees. The majority of the tests reported were conducted spanning from late September to the beginning of March of the next year, during which foliage conditions changed according to the seasons (see Figure 2(b)); the effect of foliage [27] will be evaluated in this study. Vehicle traffic was light during the day time when all the tests were conducted. During all the tests, there were about five cars per minute on the two main streets of Jenkins Avenue and East Constitution Street as shown in Figure 2(a), while there was about one car every 10 min on the other streets in the vicinity.

The building that houses the Fears Lab was constructed during the 1970s. As shown in Figure 2(c), there is one high bay area with a strong floor on its west side, while an attached office area is on its east side. All the functional areas are specified in the figure, which will be used later when evaluating the effect of rotating machinery and human activities. The high bay area is a steel structure 24 feet high with an 8-in thick concrete masonry unit (CMU) wall around the high bay area from the ground up until the height of 8 feet. Above that, there is a 0.042-in thick steel sheet wall (see Figure 2(d) and (e)). An air-conditioned chamber is located inside the high bay area at its southeast corner where the shake table used in this study is bolted down to the strong floor (see Figure 2(d)–(f)). The chamber has the same CMU wall that is 8-in thick. All the steel furniture in this chamber, which technical staff and students use to prepare their laboratory work, is also indicated in the figure. This steel furniture, which is expected to affect the performance of the packet delivery to a certain degree, was not removed from the testing site. The roof of the building is made of 2.5-in thick timber elements with a 10-in insulation layer attached underneath (see Figure 2(e)). All of these building materials may affect the transmitting range of the wireless channel. Note that there are two wireless routers mounted on the wall, one inside the testing chamber and the other in a nearby office (see Figure 2(d)). These wireless routers were kept on throughout the testing except in Section 5.4 where the effect of the 802.11b



DOI: 10.1002/stc

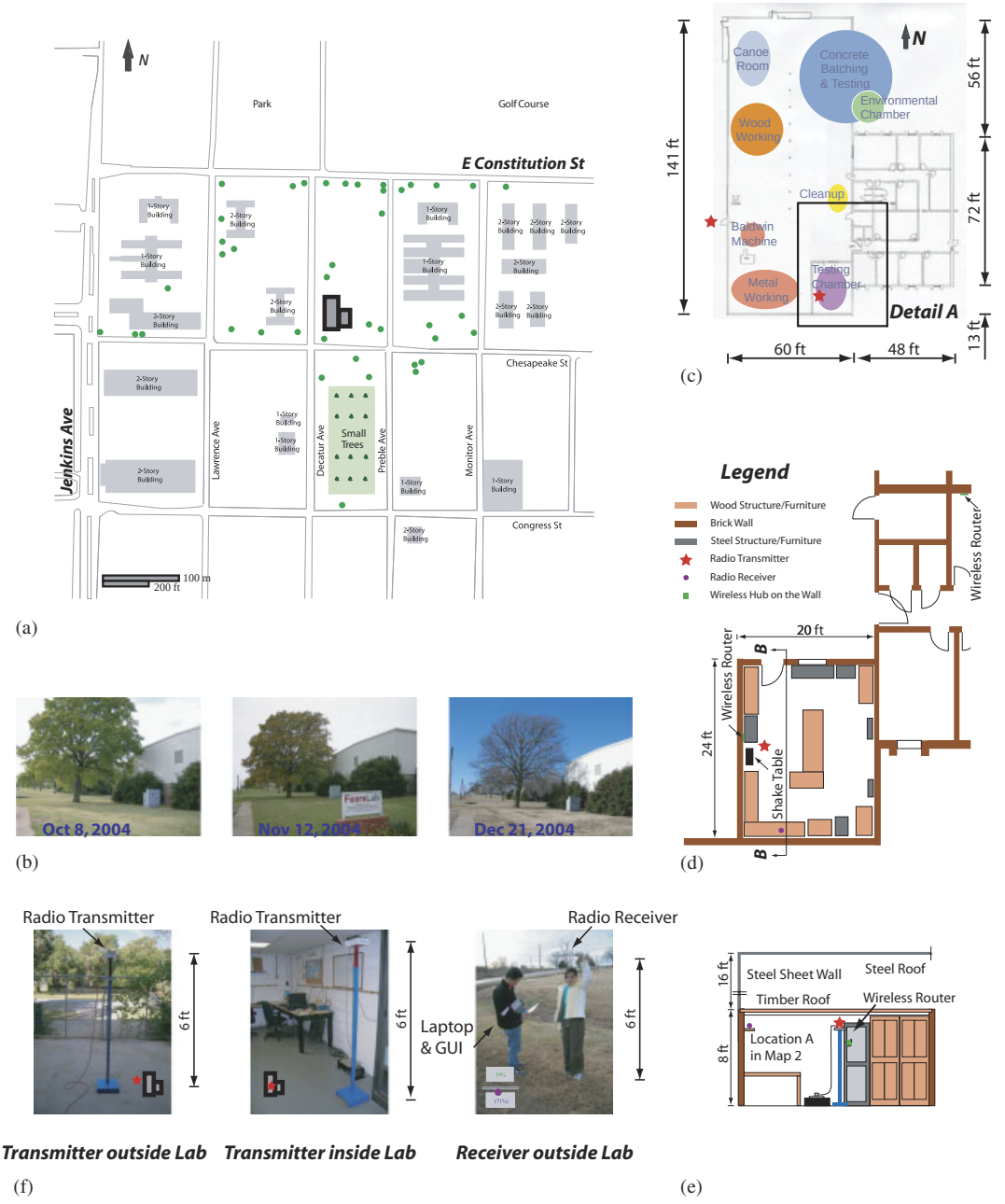


Figure 2. Details of the laboratory building and information on how signals were transmitted and collected: (a) location of Fears lab; (b) changing foliage condition; (c) plan view of Fears lab; (d) Detail A—plan view of testing chamber; (e) Section B–B—testing chamber; and (f) setup of transmitter and receiver.



DOI: 10.1002/stc

system on the 2.4 GHz radio was studied. Such a decision was made not only based on maintaining the routine research and teaching activities at the laboratory but also because of the interest of examining the performance of the designed wireless unit operated in a real-world situation. The entire experimental study, including preliminary efforts, was carried out on days of good weather (either sunny or partially cloudy) and with a roughly constant low humidity; all the tests were conducted during the daytime when there was little activity in the high bay area except in Section 5.5 where the effect of research activities, especially the use of rotating machinery and other human activities, was studied.

For this specific testing environment, the causes for packet loss and subsequent data loss may be summarized as follows:

1. Beam divergence as the signal spreads away from it source, i.e. the influence from transmitting range (the effect is governed by Equation (1)).
2. Attenuation caused by building materials (i.e. walls, roofs, columns, and beams).
3. Multipath interference.
4. Inter-channel interference (i.e. interference from a 2.4 GHz IEEE 802.11b wireless network).
5. Signal attenuation from tree foliage in the surrounding area of the laboratory.
6. Interference from vehicles.
7. Interference from other human activities.
8. Attenuation caused by other reasons, for example, rotating machinery.

Among the causes listed above, some factors are relatively permanent (e.g. Item 2) while some are changing (e.g. Items 5 and 6) or may be considered as random (e.g. Items 4 and 7). Some effects can be quantified (e.g. Item 1) as studied in various theoretical and empirical equations for path loss [7, 8] while others are harder to quantify (e.g. Items 7 and 8). It is of practical interest to differentiate between these various causes and identify the dominating factors for the sake of developing robust communication protocols and system identification methods associated with wireless sensing-based structural health monitoring.

## 3. DESIGN OF A MODULAR WIRELESS SENSING UNIT

### *3.1. Overview of hardware design*

To explore the communication reliability associated with wireless sensors within civil engineering structures, a low-cost wireless sensing unit is designed. A key feature of the wireless sensor hardware design is that it is highly modular; in other words, three ADCs are included (with resolutions 10-, 12-, and 16-bits) and two radios can be used (one operating on 900 MHz and the other on 2.4 GHz) [28]. The overall design matrix of the academic prototype wireless sensor is given in Table I while graphical illustrations are given in Figure 3.

### *3.2. Off-the-shelf radios*

There are two operational options when operating wireless radios: *batch mode* and *stream mode*. In batch mode, both the server and client start with opening their respective communication ports. The server (receiver) first sends a request for data to the client (transmitter). Upon such a request, the client samples an entire time history, then sends it through the radio. Once the data



DOI: 10.1002/stc

Table I. Hardware design details in this study [28].

| Component | Commercial brand | Description |
|---|---|---|
| Low pass filter (LPF) | Not applicable (academic prototype) | A fourth-order Butterworth filter |
| Analog-to-digital converter (ADC) | ADS8341 [29] | For 16-bit resolution |
| | ADS7841 [30] | For 12-bit resolution |
| | TLV1504 [31] | For 10-bit resolution |
| Microcontroller | Motorola 68HC11 development board [32] | Mounted on board includes 32 KB SPRAM and 32 KB EPROM |
| Radios | (1) MaxStream 9XStream (900 MHz) [33] | (1) An indoor range of 457 m with a $\frac{1}{4}$ wave monopole whip antenna and 140 mW transmit power output |
| | (2) MaxStream 24XStream (2.4 GHz) [33] | (2) An indoor range of 183 m with a $\frac{1}{2}$ wave dipole antenna and 50 mW transmit power output |

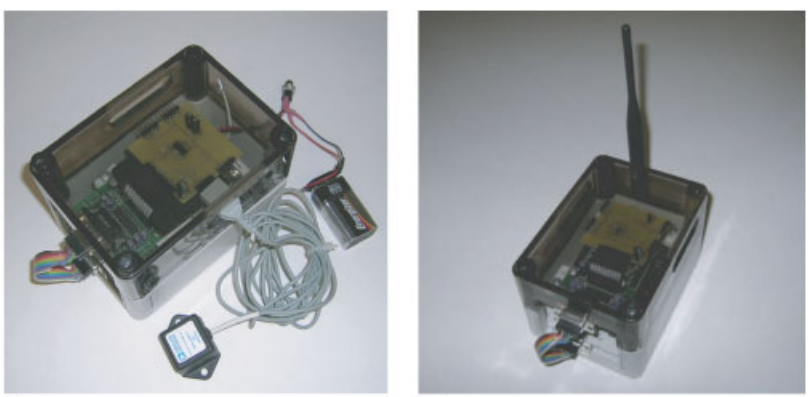


Figure 3. Developed wireless unit with: (a) a MaxStream 9XStream radio (900 MHz), the attached ADXL105EM-1 MEMS accelerometer, and a 9 V battery and (b) a MaxStream 24XStream radio (2.4 GHz) [28].

are received, the server stores the data internally, closes the communication port and then proceeds with its data display tasks. Note that handshaking occurs only once to synchronize the transmitting and receiving radios. Stream mode is similar to the batch mode except having numerous iterations of making a request, receiving data, and storing data at the server for *every* data point (DP). In other words, handshaking occurs often during the transmission of an entire time history to keep client and server synchronized. The entire time history is sent point by point under this mode.

To ensure wireless data transmission is near real time, batch mode rather than stream mode is a preferred option in this study. This is because handshaking could take upwards of 45 ms for each transfer, which would lead to a long waiting time to deliver the entire time history under stream mode. In addition, there are no 're-try' operations in this study because an acknowledge or retry (ACK/NCK) protocol is *not* adopted. The time saved from not using 're-try' operations is tremendous. For a shake table test to be presented in Section 4.2, a time history was received



DOI: 10.1002/stc

within 1 min after the request was made at the server when operating in batch mode. The 'one time' wireless data transmission maximizes the throughput of data and minimizes the latency of communication. The price to achieve this near real-time wireless data channel is its more challenging reliability performance.

### *3.3. Software design*

The design goal of the embedded software used to automate the operation of the wireless sensing unit is to ensure that data is properly delivered from a wireless transmitter to a receiver. For the wireless sensing unit sending data in near real time, it is important for the receiver to receive, display and store data in the correct sequential order that data were transmitted. Towards this end, a flexible payload size scheme, which is default in the selected XStream radios, was adopted. In addition, a robust error check algorithm was developed to accurately reconstruct the signals at the server.

A *flexible payload scheme* was adopted instead of a *fixed payload scheme* in this study. As the names imply, the main difference between these two schemes is whether the payload (i.e. the core information in a radio packet) has a fixed number of bytes. For example, a flexible payload might have '$n$' bytes during one packet transmission while the next transmission might have '$m$' bytes. As commonly seen in wireless communication [9], a flexible payload scheme offers increased throughput and reduced latency of the transmission, which is a clear advantage over a fixed payload scheme. A flexible payload scheme was offered by the MaxStream radios [34], while the fixed payload scheme was not available to MaxStream users [35] at the time of the study. The downside of adopting a flexible payload scheme is the issue of partial packets, which refers to the uncertainty in assigning DPs to radio packets; in other words, a radio packet can contain more than one DP and even partial DPs. The challenge caused by partial packets has been extensively studied in the wireless communication field (e.g. [36]). Such a partial packet problem was addressed in this study with an error check algorithm developed for signal reconstruction at receiver end.

To elaborate more on the flexible payload design option, the relationship between radio packets and DPs is depicted in Figure 4. The structure of an idealized packet containing one DP is shown in Figure 4(a) where the first byte is a microcontroller header byte (MHB) followed by two bytes for a packet ID (PID) and then another two bytes used for the value of the DP. Packet IDs are simply successive sequential numbers of the packets generated at the client end; they were introduced to allow the server to locate the position of any lost data in a received time history. In this study, the maximum data set length is limited to 12 000 measurement points due to the limited memory of the selected Motorola 68HC11. This requires a 16-bit packet ID field since 8 bits would only allow a maximum of 256 unique packet IDs, while 16 bits allow a maximum of 65 536 unique packet IDs. At the transmitter, the packets are sent to the radio through a serial port and stored in a radio buffer before communicating. A header and cyclic redundancy check (CRC) are added to each radio packet before the transmission as shown in an idealized radio packet in Figure 4(a). CRCs are used to detect errors after the transmission.

The selected XStream radios allow the packet to vary between one byte to 64 bytes [34]. Figure 4(b) shows an example of three radio packets containing five DPs to represent a typical situation when a flexible payload scheme is used. At the receiving end, the radio decodes the received packets and checks their errors using the CRC. When the second packet fails the CRC as shown in Figure 4(c), the developed error check algorithm will drop *all* the data



DOI: 10.1002/stc

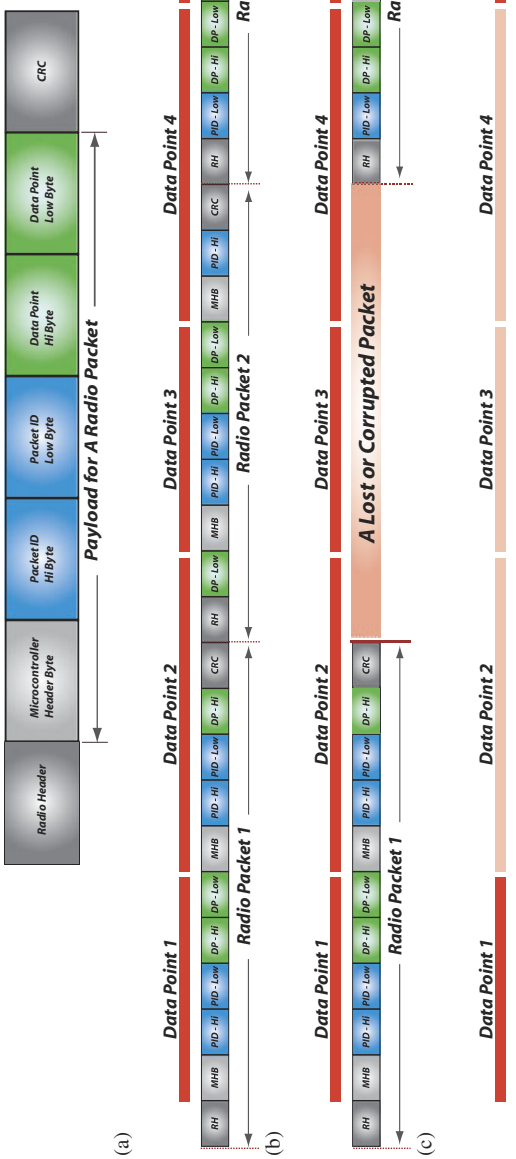


Figure 4. Illustrations of the relationship between radio packets and data points (DPs) by using the adopted flexible payload scheme and the developed error check algorithm: (a) an idealized packet structure for a single data point; (b) an example of an assembly of three consecutive radio packets and the corresponding five consecutive data points to be transmitted; (c) an example of possibly received radio packets with packet loss; and (d) the reconstructed data points with data loss. (Note that dark colour denotes received data points.)



DOI: 10.1002/stc

(both complete and partial DPs) associated with this packet, i.e. DPs 2–4 as shown in Figure 4(d). When a DP is not received, a value of zero is assigned in the time history. Therefore, three zero values will be assigned to DPs 2–4 in this example, while the values of the remaining DPs (DPs 1 and 5) are preserved.

Such an error algorithm was tested to be robust even with a modular hardware design, namely three ADCs with different resolutions [28]. In addition to the error check algorithm developed at the receiver, another key feature of this implementation is not to store the packet IDs in the transmitting node memory but only generate them for the purpose of transmission. This technique used the available client memory only for storing the data sets received from the ADC and therefore is highly optimized.

## 4. OVERVIEW OF EXPERIMENTAL INVESTIGATIONS

The experimental investigation reported in this paper is considered in two parts as outlined in Table II. In Part I, loopback tests were conducted using the XStream radios. These tests examined the transmitting range of the radios and characterized the transmitting environment. Based on the results of Part I, time histories of shake table tests were collected at several locations that would result in different degrees of packet loss using the 9XStream radio. Patterns of data loss are then examined at these locations. For the 24XStream radio, its performance is examined by collecting the same shake table time histories at an indoor location with the focus

Table II. Testing matrix in this study.

| | Part I: loopback | | Part II: shake table | |
|---|---|---|---|---|
| Testing condition | 9XStream | 24XStream | 9XStream | 24XStream |
| Radio | | | | |
| Transmitter location | | | | |
| Outside Lab | 1 (Map 1*) | 1 (Map 3*) | NA | NA |
| Inside Lab | 1 (Map 2*) | 1 (Map 4*) | 1 | 1 |
| Receiver location | | | | |
| Outdoors | 12 (Maps 1 and 2*) | 12 (Maps 3 and 4*) | 5 (Locations B to F in Map 2*) | NA |
| Indoors | NA | NA | 1 (Location A in Figure 2(d) and (e)) | 1 (Location A in Figure 2(d) and (e)) |
| Sets of transmitting range | 24 | 24 | 5 | 1 |
| Building material attenuation | Considered | Considered | Considered | Not considered |
| Inter-channel interference | NA | Considered | NA | Considered |
| Other attenuation factors | Considered | Considered | Considered | Partially considered |
| Different ADC resolutions | NA | NA | 10/12/16-bit | 12/16-bit |
| Different sampling rates | NA | NA | $f_s = 500$ Hz<br>$f_s = 100$ Hz | $f_s = 500$ Hz<br>$f_s = 100$ Hz |
| Transmitted time-history length | NA | NA | 12 000 | 12 000 |

*Refers to the four maps in Figure 5.



DOI: 10.1002/stc

on examining the interference from an active 802.11b system in the environment (also operating on 2.4 GHz). All of these shake table tests are presented in Part II.

In this study, the wireless sensor unit is used as the *transmitter* (or, *client*) and a laptop as the *receiver* (or, *server*). Shown in Figure 2(d)–(f) is the set-up of the transmitter and receiver. Based on the concept of the Fresnel zone [37] (i.e. a profile of wireless signal transmission path between two antennas), the antennas should normally be mounted well above the ground to avoid a reduction in the transmitting range caused by interference of the central diameter of the Fresnel zone by the ground. In this study, a steel post was designed to place the transmitter 6 feet off the ground. Similarly, the height of the server was approximately 6 feet off the ground. Thus, it can be considered that $h_t = h_r = 1.83$ m in some propagation models (e.g. [7]) for this study. A timber post was at one time used to replace the steel post to support the wireless unit at the client end. There were no obvious difference caused by using a timber post, thus the steel post was used throughout this experimental study. Also shown in Figure 2(f) is a laptop used on the receiver side to communicate with the transmitting wireless sensing unit. Since the wireless sensing unit must remain mobile, it was powered by a simple 9 V DC battery.

### *4.1. Part I: radio loopback tests*

Investigating the packet delivery performance is considered the foremost step in studying the quality of the wireless channel used by the developed wireless unit. In terms of terminology (e.g. [6]), *packet loss rate* means the fraction of the packets not received or not successfully passing the CRC. The complementary quantity of packet loss rate is *packet reception rate*. Loopback tests are commonly used as an initial test to diagnose failing nodes in a network. A loopback test is one in which a signal is sent from the server/receiver to the client/transmitter and then looped back to the original server/receiver using a special plug with the selected XStream radios [33]. In this study, loopback tests were adopted as a fast field testing method to characterize the selected transmitting environment, where the attenuation of the wireless signals is due to the combined effects of many factors aforementioned in Section 2.2. Loopback tests were carried out at different laptop locations that corresponded to different transmission ranges while the wireless sensing unit was fixed at a location either inside or outside the Fears Lab (see Figure 2(c) and (f)). At each laptop location, the loopback test was repeated four times to obtain an average value of a packet reception rate. Each time, the laptop radio transmitted 100 packets, each 32 bytes in size, to the wireless sensing unit radio, which in turn returned all the received packets to the laptop radio. The software operating at the laptop counted all the good packets that it had received. The results are presented in Section 5.1.

### *4.2. Part II: shake table tests*

Shake table tests were the primary focus of this experimental study. Time histories of vibration data were recorded by an accelerometer mounted to the top of a shake table and transmitted to examine data delivery performance of the developed wireless unit. To examine the severity of data loss and loss patterns present within the transmitted time histories, six laptop locations (one indoor and five outdoor corresponding to different transmitting ranges) were selected to collect the time histories while the wireless sensing unit was always fixed indoors, i.e. at the location of the shake table (see Figure 2(d)–(f)). Furthermore, numerous combinations of hardware design configurations (e.g. ADCs of 10-, 12-, and 16-bit resolution) and operational



DOI: 10.1002/stc

conditions (e.g. sampling rate $f_s = 500$ Hz and $f_s = 100$ Hz, respectively) were employed at each location to study their effect upon the quality of the collected data and processed results.

In this study, an electromagnetic shake table was used to generate vibration signals. An empty shake table was instrumented with an accelerometer at the centre of its top plate. The shake table is used to simulate data anticipated from a dynamic structure. An analog accelerometer, ADXL105EM-1 from Analog Devices [38], was used in 0–5 V single-ended mode. A 12-bit arbitrary waveform generator card [39] from National Instruments was used to generate a periodic swept sine excitation to drive the empty shake table. The swept sine started at 0.10 Hz and ends at 20 Hz with a duration of 15 s. The data length was unified to be 12 000 for all the collected time histories. Such a data length permitted the recording of one full period of the response of the shake table even at sampling rate $f_s = 500$ Hz.

The case of using the same ADXL105EM-1 accelerometer interfaced to a tethered data acquisition system (i.e. a 'wired' case) was employed as a control experiment where sensor data were collected using a 16-bit NI DAQCard-6036E [40]. The response recorded by the tethered data acquisition system was used to to assess when data were lost in the wireless system. For other tests when the wireless unit was used, the server (laptop) inserted an artificial '0' *in lieu* of the true DP(s) wherever data loss occurred. A time history collected by the server could be readily converted into another one showing a blank spot for a lost DP. The *data reception rate*, which is simply the percent ratio of the number of received DPs to the total number of DPs in a time history, was then calculated.

## 5. RESULTS AND ANALYSIS

### 5.1. Results of loopback tests

All the results of the loopback tests are presented in Figure 5, where the four maps show the same area but with different testing results that can be used to evaluate the roles played by these *four factors*: (1) the transmitting frequency and power of the radios; (2) transmitting range; (3) effect of building materials; and (4) foliage attenuation. In detail, Maps 1 and 2 are for the selected 9XStream radio (900 MHz), while Maps 3 and 4 are for the 24XStream radio (2.4 GHz). The wireless sensing unit (i.e. the transmitter/client side), shown by a star, was outdoors in Maps 1 and 3, and indoors in Maps 2 and 4, respectively. The loopback test was conducted along four main directions (north, south, east, and west). In the maps, the multiple laptop (i.e. the receiver/server side) locations are highlighted as dots and indicated with the average packet reception rates based on the sent 400 packets (100 packets repeated four times). Two sets of the results on each map were from the tests in two seasons (i.e. with different foliage conditions). The first set, the values of which are without parentheses, were recorded in early fall. The second set, whose values are inside parentheses, were recorded in winter.

Before commenting on the results in Figure 5, it is important to bear in mind that each reception rate value is the mean of received packets when 400 packets are sent. To better illustrate the behaviour of packet delivery as a function of range, trends in these results are sought from all four maps in each direction (north, south, east, and west) as shown in Figure 6. As Equations (1) suggests, the power of a wireless signal reduces with range following a power function; as such, the quality of the channel, as represented by reception rate, would also follow a power function. For a given radio (9XStream versus 24XStream) along a given direction, it



DOI: 10.1002/stc


Figure 5. Results of loopback tests of MaxStream 9XStream radio (900 MHz) (in Maps 1 and 2 at the left column) and 24XStream radio (2.4 GHz) (in Maps 3 and 4 at the right column). The values without parentheses were recorded in fall, while the values inside parentheses were recorded in winter.

can be seen that the power decaying relationship between packet reception rate and transmitting range holds for the majority of the tests results. The east and west directions when the 24XStream radios were used, however, exhibit abnormal trends. At this point, it is hypothesized



DOI: 10.1002/stc

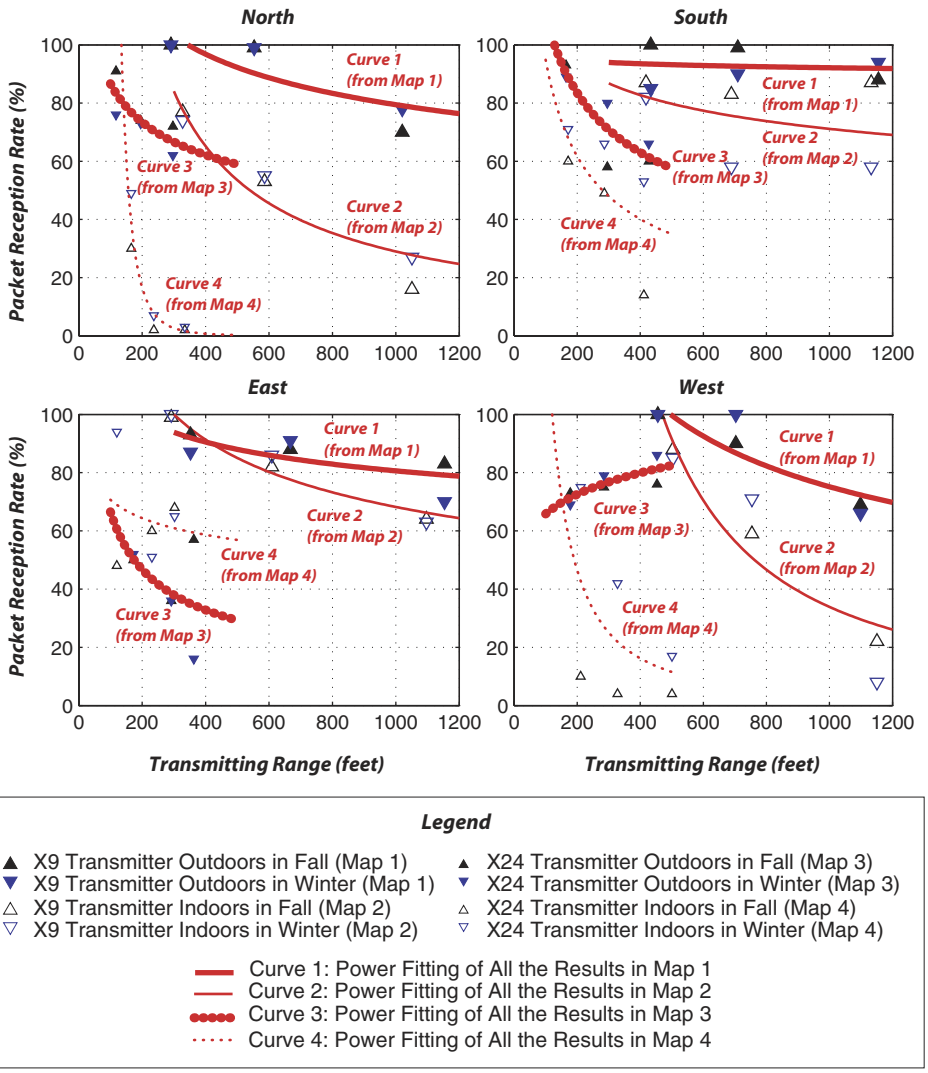


Figure 6. Relationships between packet reception rate and transmitting range along four directions obtained from Figure 5. Note that the curves are fitted according to an assumed power relationship following Equation (1). Large extrapolation is avoided in presenting these curves.

that these unexpected trends are caused by multipath effects and inter-channel interference. Clearly, more receiver (or server) locations should be adopted in future studies to provide a greater density of data that can be used to refine the trend lines established in Figure 6.

Maps 1 and 2 in Figure 5 and Curves 1–4 in Figure 6 give a qualitative idea of the role played by transmitting range, effect of building materials, and foliage attenuation. The two maps have identical sets of laptop locations (and roughly the same transmitting ranges) but different wireless sensing unit locations. In Map 2, six locations are specified from A to F;



DOI: 10.1002/stc

these are the locations where the time histories of shake table vibrations were collected (the result of which are presented in the following sections). It can be seen from the four curves that the behaviour of the wireless communication channel is roughly as expected; reception rate falls off with distance and putting the transmitter inside the building causes a decrease in the reception rate.

The important role the radio plays can be easily seen by comparing the results between Maps 1 and 3, and 2 and 4 in Figure 5 and the corresponding curves in Figure 6. In addition to the difference in carrier frequency, the MaxStream 9XStream (900 MHz) and 24XStream (2.4 GHz) radios differ in terms of transmitting power [33] and the attached antenna (see Table I). Note that the data were collected at shorter transmitting ranges when the radio of a higher frequency and lower transmitting power was adopted. This adjustment is necessary first because of the inter-channel interference caused by the two operating wireless routers inside Fears lab to the transmission of the MaxStream 24XStream radio. More importantly, there is a drastic difference in terms of transmitting range between 9XStream (900 MHz) and 24XStream (2.4 GHz) radios. With a longer wavelength, the 900 MHz radio exhibits better propagation properties since longer wavelengths allow wireless signals to bend corners and propagate more easily past physical obstructions. In contrast, as the frequency of the wireless signal increases, it behaves more like visible light (which is also a high-frequency signal) where LOS obstructions can stop the signal. This is consistent with the 2.4 GHz radio which is more sensitive to the obstruction shown in Figure 5.

More qualitative conclusions about the building material attenuation can be drawn as follows. Note that similar conclusions can be drawn from Maps 3 and 4.

1. Along each of the north, west, and south directions, the packet reception rate was reduced distinctively when the transmitter was moved from outside (Map 1) to the inside of the lab (Map B). This can be explained by the addition of the walls of Fears lab that the signals had to penetrate in the later condition. In most of the receiver locations, the packet delivery performance of the east direction was affected adversely when the transmitter was moved from the outside (Map 1) to the inside (Map 2). This is largely because of the increment in the number of walls that the signals had to penetrate in the later condition.
2. As shown in Map 1, the transmission in the north and south directions was close to LOS. Accordingly, the packet delivery performances along both directions were consistent. However, this consistency did not hold in Map 2. The reduction in the packet delivery performance was less along the south than that along the north direction. This is likely due to the transmission along the North direction in Map 2 was blocked by a larger number of walls than that along the south direction as shown in the plan view of Fears lab in Figure 2(c).
3. The more severe reduction in the packet delivery performance along the west direction in both Map 1 and 2, as compared to the south direction can be similarly explained as above due to an increased number of walls/roof, again adding more evidence for the strong effect of the attenuation from building materials.

The difference between the results collected in fall and winter is not consistent, which suggests that foliage attenuation, for this specific transmitting environment, was a minor factor in packet loss. Therefore, the four curves are derived in Figure 6 by averaging out the results obtained in fall and winter.



DOI: 10.1002/stc

### 5.2. Relationship between results of shake table and loopback tests

Six laptop locations were selected to measure the performance of data transmission by using the periodic time histories generated by the shake table; their locations are indicated as Locations A–F in Map 2 of Figure 5. These locations were *not* chosen solely based on transmitting range. Rather, the loopback test results in Map 2 were used to distribute these server/laptop locations for anticipated packet delivery rates ranging from about 90 to 50% from Locations B–F, respectively. In particular, Locations B and D had similar transmitting ranges but drastically different loopback results. Uncertain environmental factors might contribute to this difference; however, building material attenuation seemed to be the leading factor as analysed in Section 5.1. Location E had the farthest transmitting range; however, its loopback reception rate was not the lowest. Location A, a new location entirely for the shake table tests, is indicated in Figure 2(d) and (e) with a transmitting range of about 14 feet. Location A was expected to yield the best performance using the wireless unit since it was an indoor location and LOS to the client.

Throughout the shake table tests, data loss rather than packet loss was studied. First, this is because of the driving interest in this study of focusing on data interpretation and system identification (see Section 1, especially Figure 1) rather than studying packet delivery performance. The second reason is that the selected off-the-shelf radios were programmed to directly identify data rather than packet delivery performance (see Section 3.3). As shown previously in Figure 4, no one-to-one mapping exists between a packet and DP in the flexible payload scheme; a packet can contain an uncertain number of DPs. Moreover, a packet can contain an incomplete DP. As a potential end-user of wireless sensing, one would desire to estimate the severity of data loss based on a fast prototyping test like a loopback test as shown in Figure 1. Thus, this section attempts to relate the results from these two sets of tests (loopback *versus* time-history transmission) to each other. In other words, the feasibility of predicting data loss rate (as pertinent in the shake table test) based on an easily measured packet loss rate (obtained from the loopback tests) at the same location is explored. If the loopback test results accurately predict the loss of data during the shake table tests, then this suggests the loopback test can be used during the installation of a wireless monitoring system to select 'optimal' locations to install wireless sensors (where optimal implies minimal data loss).

Figure 7 presents the *data reception rates* calculated from the shake table tests overlaid with the *packet reception rates* from the loopback tests collected at the same server locations. In total, 54 data reception rates, each consisting of 12 000 transmitted points from the shake table tests are presented in the figure for each location ID. It can be seen that the dispersion of these rates at the indoor Location A (of zero loss) is zero, which is the least of all the cases. At other outdoor locations, the reception rates vary in a range of about 15–35% at the same location. In Figure 7, the legend used indicates the test repeated for data collected using the three different ADC resolutions (10-, 12-, or 16-bit) all sampled at 500 Hz. The different ADC configurations are not expected to impact the packet delivery performance. However, environmental factors including foliage, traffic flow, and human activities will affect packet delivery performance and subsequent data loss. Data consecutively collected at the same location on the same day (i.e. the three samples at the same location under the same configuration) have a dispersion of data loss of less than 25% in all outdoor cases, which is smaller than the range described above that includes tests done at the same location but on different days. This loosely demonstrates the influence a wide range of environmental factors has on data delivery performance.



DOI: 10.1002/stc

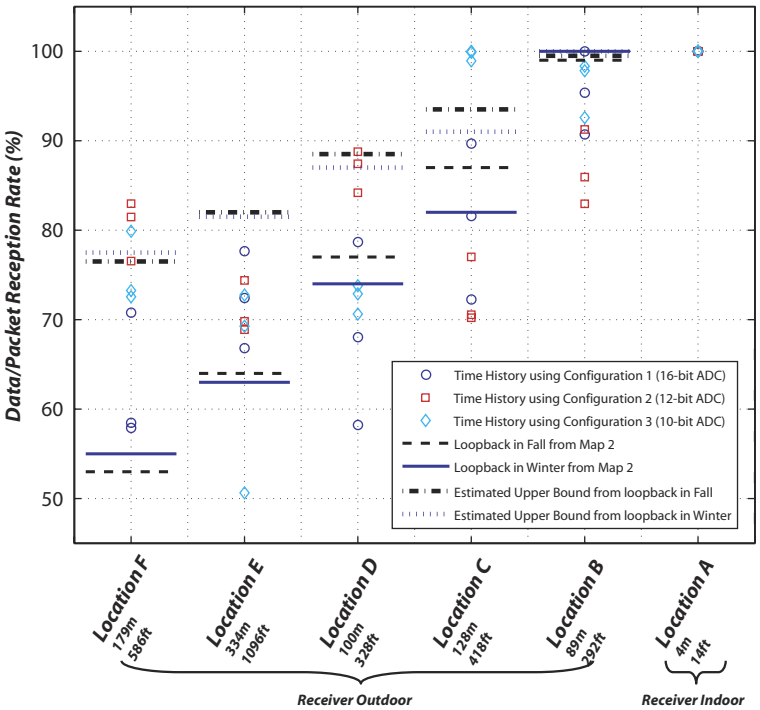


Figure 7. Data/Packet reception rates calculated from transmitted shake table time histories and those based on loopback tests. (The values of transmitting range for each locations are indicated in the figure.) The loopback results are adopted from Map 2 in Figure 5. The estimated upper bound is obtained by assuming equal rates for both ways of transmission in a loopback mode, while the original value of packet loss in two-way communication represents a lower bound.

The packet reception rate is calculated from loopback tests where the transmitter sends a packet to a receiver which instantly loops it back to the transmitter. As a result, the rate is based on *two-way* communication. If it is assumed an equal probability of a lost packet in both communication paths, then an estimated packet reception rate for *one-way* communication would be one minus one-half of the packet loss rate. This adjusted reception rate will be referred to as an *upper bound* on the packet reception rate. As shown in Figure 7, the loopback packet reception rate and the upper bound packet reception rate are overlaid with the data delivery rate obtained during the shake table test.

Again, it is important to note the differences between these two sets of receptions rates. A loopback test yields a packet reception rate from a loopback mode following a fixed payload size scheme [33], while the one-way transmission-based shake table test leads to a data reception rate by using a flexible payload size scheme. As stated previously, such a scheme will minimize network latency and optimize throughput at the price of assigning an arbitrary number of DPs to a packet thereby worsening consecutive data loss. Strictly speaking, these two sets of rates are different quantities although they are closely related to each other. Furthermore, the results from the loopback tests in this study took an average of only 400 packets. In contrast, each transmitted time history contained 12 000 DPs. Nevertheless, the major connection between



DOI: 10.1002/stc

these two sets of results is that they are affected by the same transmitting range and similar environmental conditions. This exercise suggests the possibility of adopting the loopback as a fast prototyping method for characterizing a transmitting environment, although more realizations of the random process need to be collected and further theoretical and/or simulations are needed to justify and refine this practical approach.

### 5.3. *Received shake table time histories*

Typical time histories received at locations A through F using the 9XStream radio (900 MHz) at a sampling rate $f_s = 500$ Hz are shown in Figure 8. It can be seen clearly that the lost data tends to cluster in time. This phenomenon imposes a challenge for numerical interpolation schemes used to recover missing DPs, especially for the locations where the signal loss is frequent. Data loss with a similar clumpy feature is also observed for the 9XStream radio (900 MHz) at a sampling rate $f_s = 100$ Hz and the 24XStream radio (2.4 GHz) at both sampling rates. Detailed analysis will be presented in Section 6 to reveal the underlying stochastic features of those losses leading to better understanding of their nature and potential technical solutions that minimizes their impact.

### 5.4. *Effect of wireless routers on the 24XStream Radio* (2.4 *GHz*)

For the selected MaxStream 24XStream radio (2.4 GHz), two 802.11b routers inside Fears lab (see Figure 2(d) and (e)) are expected to affect the signal transmission due to inter-channel interference. The existence of a 2.4 GHz wireless network could be typically encountered when installing a structural health monitoring system due to the widespread existence of such internet technologies in buildings. Unlike all the shake table tests using the 9XStream radio, the unique focus for designing all the tests using the 24XStream radio is to study inter-channel interference while keeping the transmitting condition simple as shown in Table II.

Two sets of tests were conducted to study such an effect. In the first set of tests, the shake table vibration data were collected at Location A (see Figure 2(d)) when the wireless router at the remote location was left on throughout the test (since it is a main router used by the entire laboratory) while the wireless router inside the testing chamber was alternatively turned on and off. Such a test was expected to reveal the impact of inter-channel interference; when the nearby wireless router was turned off, the inter-channel interference was only from the remote router, while the interference was from both the routers when the nearby router was turned on. The results indicate that the effect from both routers was in general more severe than that from a remote one only, although the results show a large fluctuation in data reception rate from all the cases as will be presented later in Section 6. For example, using the 2.4 GHz MaxStream radios, the average and standard deviation of the data reception rates of the collected time histories at $f_s = 500$ Hz are 76.66 and 17.96%, respectively, when the nearby router was on, and are 97.39 and 2.01%, respectively, when the nearby router was off.

In the second set of tests, both wireless routers were turned off to examine the best performance of the selected MaxStream 24XStream (2.4 GHz) radio. During one evening when there were no activities at Fears lab, the shake table vibration data were collected using the 2.4 GHz radio at Location A. It was found the data reception rate calculated from the 11 received time histories was 97.62% on average, while the loopback tests conducted at the same location right after the shake table tests gave an average packet reception rate of 84% (lower bound) based on 400 packets (which leads to an estimated one-way packet rate of 92%



DOI: 10.1002/stc

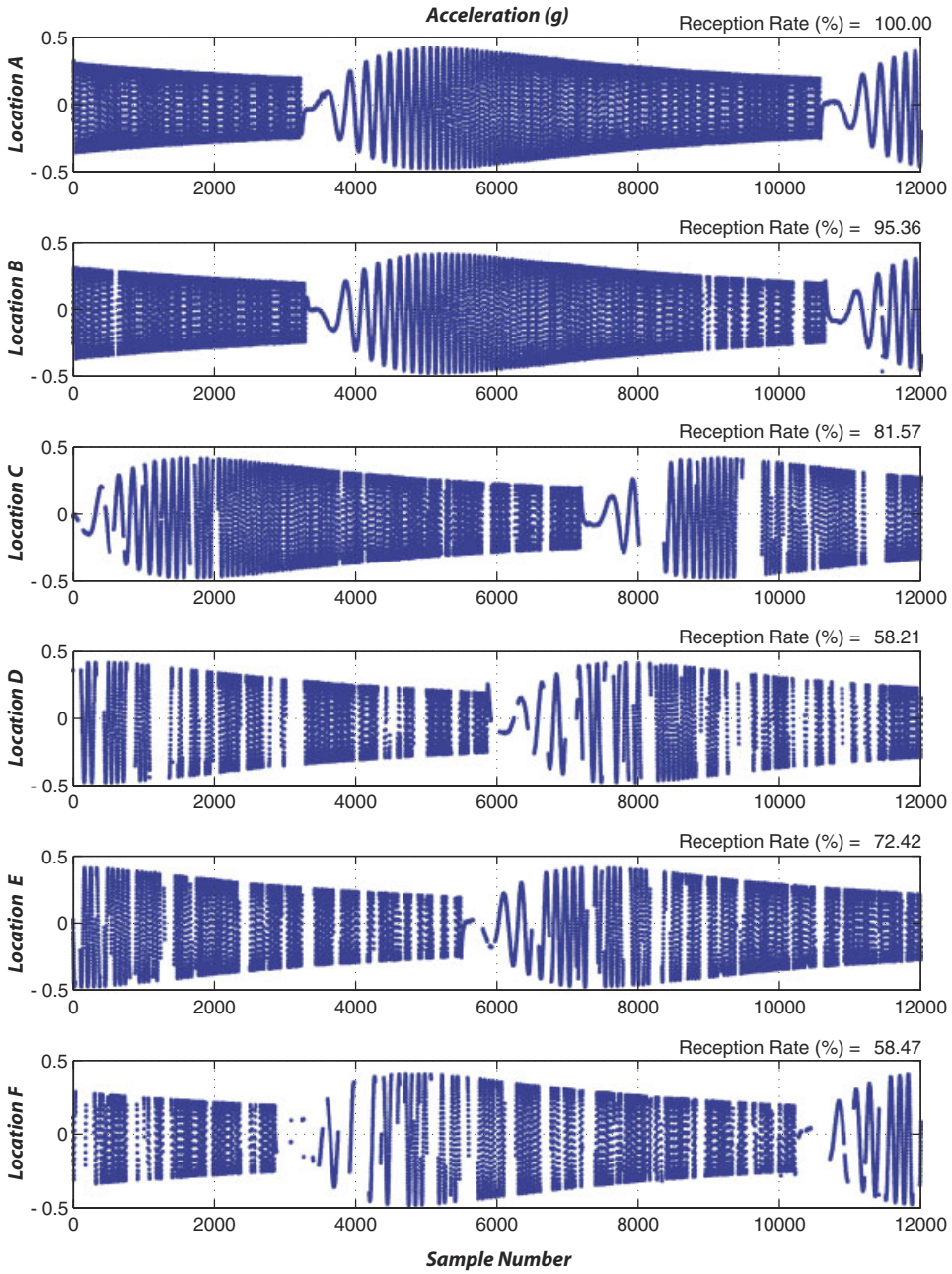


Figure 8. Time histories of sample set *b* using ADXL105EM-1 and 16-bit ADC with LPF, 9XStream radio and sampled at $f_s = 900$ MHz from Locations A–F with a decreasing anticipated reception rate from 100 to 50%. Note the reception rates calculated from each measured time histories are indicated on the top right corner of each panel.



DOI: 10.1002/stc

according to Section 5.2). Recall the transmitting range for Location A was 14 feet and the condition was LOS; the reason for packet and data loss is the low transmitting power of the selected 2.4 GHz radio (50 mW). Another 2.4 GHz radio from Aerocomm [41] with a transmitting power of 100 mW was adopted in the test at the same location in the same evening, it yielded no packet and data loss when both the routers were turned off.

### 5.5. *Preliminary study on effect of rotating machinery and human activities*

Supplementary to the main experimental study reported, the effect of rotating machinery and human activities was briefly explored in a summer month when there was ongoing experimental work at Fears lab involving heavy machines (e.g. for welding, sawing, drilling and grinding steel specimens and batching of concrete). See Figure 2(c) for the functional areas of Fears lab. Throughout these preliminary tests, the shake table was still used to generate the same periodic signal.

For the 900 MHz radio, several tests showed that the influence from these activities was negligible when the time histories were collected at Location A. On one occasion, the data reception rate was lowered to 74.38% from an operating concrete mixer when the shake table time histories were collected at Location B. Note that there was approximately a LOS condition between the location and the mixer.

For the 2.4 GHz radio, supplementary data sets were collected entirely at Location A when the nearby wireless router was turned off and on from time to time. The results, however, do not show consistent impact from rotating machinery outside the chamber under the specified testing configuration, i.e. the effect of operating machinery can either be hardly told or hard to explain. However, it seems to be consistent that crowds inside the testing chamber did affect the data transmission. On one occasion, when the chamber was suddenly filled up with three student visitors, it was very hard to establish the initial wireless connection in addition to poor data delivery performance.

## 6. STATISTICAL MEASURES OF DATA LOSS

As outlined previously in Figure 1, studying the data loss issue will aid researchers exploring system identification and damage detection algorithms embedded within wireless structural health monitoring systems. One specific scenario would be to 'foresee' (i.e. without doing any physical testing or doing the minimum amount of testing) how original time histories collected by wireless sensors will be altered by data loss in the wireless channel. Data loss is of extreme importance when there is a need for real-time or near real-time communication such as after an extreme loading event.

To address such a research need, the time histories collected from the shake table tests will be used to derive statistical measures of data loss. Such features are critical for researchers who wish to generate artificially lossy time histories which represent time history records collected within a wireless monitoring system. Such simulated lossy time histories might be used to assess the effectiveness of extrapolation schemes or to determine the necessary condition for the completeness of data sets used in system identification and damage detection.

As will be outlined in Section 6.1, statistical analysis and random process theory are introduced first to define the *statistical measures* of data loss in a wireless channel. While mining



DOI: 10.1002/stc

the complex and seemingly random phenomenon of data loss in this context, the following possibilities are investigated to aid future prediction and simulation work:

1. Whether the same testing condition (e.g. transmitting range) is correlated to invariant loss patterns will be presented in Section 6.2.
2. Whether data loss rates are associated with invariant data loss patterns will be presented in Section 6.3.
3. It is expected that the data loss pattern should not be affected by sampling rate given the radio is operated in batch mode (see Section 3.2), which will be verified here using the data from the 24XStream radio at two different sampling rates, 100 and 500 Hz.

### *6.1. Analysis tools for time histories with data loss*

As shown in Figure 8, data loss tends to cluster in time; consecutive points of data loss are viewed as 'gaps' in a perfect time history. To approach the problem, one would need a clear picture of individual data loss clusters/gaps as well as how these clusters/gaps are distributed along a time history. To simplify the analysis, the time history records collected from shake table tests can be converted into binary signals. The value of 1 is assigned to a lost DP while for a received DP, the value of 0 is given. This specific assignment of 1 and 0 is because the central issue is data loss rather than data reception; the obtained binary signal will simplify the corresponding statistical analysis that follows. The issues to be explored include:

*Overall feature of each individual data loss cluster*: This can refer to the minimum, maximum, mean, and standard deviation of the size/width of these clusters/gaps.

*Histograms of empirical probability density functions (pdf) of the size of data loss clusters*: This would be the most quantitative description of the dispersion of individual loss clusters/gaps.

*Frequency of the occurrence of these clusters/gaps*: This would be the first step to understand the distribution of these clusters/gaps in an individual time history.

*Autocorrelation and autocovariance functions*: These are effective tools in studying stationary random processes (e.g. [42–45]) including packet delivery performance [6]. Equations (2) and (3) are used to calculate normalized autocorrelation and autocovariance functions of the aforementioned binary process in this study, where $x_n = 0$ (received DP) or 1 (lost DP).

$$R_{xx}(\tau) = \frac{\sum_{n=0}^{N-\tau-1} x_{n+\tau} x_n}{\sum_{n=0}^{N-1} x_n^2} \tag{2}$$

$$C_{xx}(\tau) = \frac{\sum_{n=0}^{N-\tau-1} \left( x_{n+\tau} - \frac{1}{N} \sum_{i=0}^{N-1} x_i \right) \left( x_n - \frac{1}{N} \sum_{i=0}^{N-1} x_i \right)}{\sum_{n=0}^{N-1} \left( x_n - \frac{1}{N} \sum_{i=0}^{N-1} x_i \right)^2} \tag{3}$$

For the time-history samples presented in Figure 8, the pdfs are presented in Figure 9(a). It can be seen that the distribution of the size/width of these clusters/gaps is neither uniform nor normal. Rather, the distribution shows multiple peaks and a long tail. Similarly, the autocorrelation and covariance functions of data loss are presented in Figures 9(b) and (c), respectively. Note that these plots demonstrate a temporal correlation of the data loss. A spatial correlation of the data loss (i.e. the cross-correlation of the data loss at different locations but at



DOI: 10.1002/stc

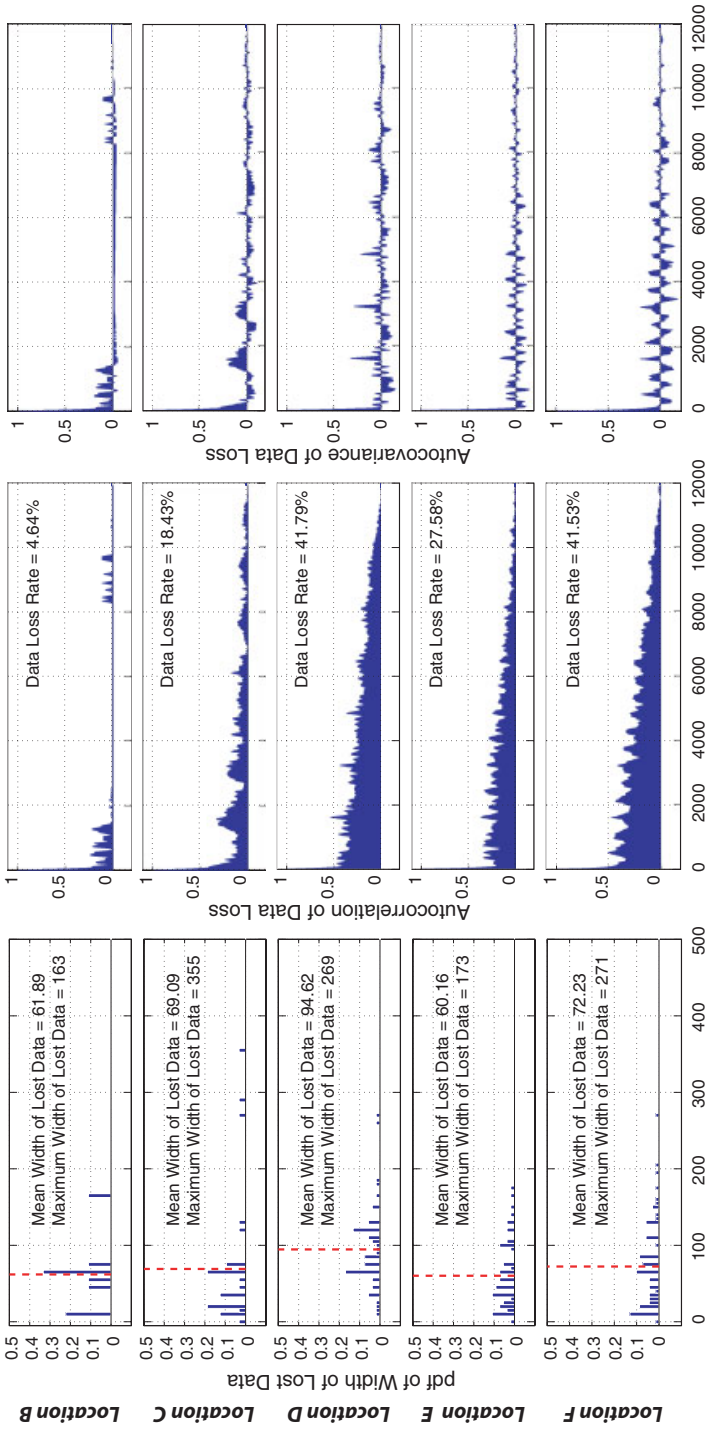


Figure 9. (a) Histograms of empirical probability density functions (pdfs) of the width of lost data of the time histories presented in Figure 8. The dashed lines indicate the average values of the width in each panel; (b) Stem plots of normalized autocorrelation of data loss; and (c) stem plots of normalized autocovariance of data loss of the same time histories.



DOI: 10.1002/stc

the same time) cannot be derived due to the limitation that only a pair of wireless sensor nodes, rather than a synchronized sensor network, was adopted in this experimental study.

It is well known (e.g. [44]) that a normalized autocovariance function of a random process should be near zero for any and all time lags except being 1 at lag 0. In contrast, a non-random process should have an autocovariance plot with significantly non-zero values at one or more time lags. All the plots in Figure 9(c) show strong correlation of the data loss, suggesting it is a non-random process. This is reasonable because of the way the error algorithm drops bad packets with consecutive DPs potentially contained in a packet (as depicted in Figure 4). This is the first important observation from both the autocorrelation and autocovariance plots. Another observation is the periodicity in the data loss; the autocovariance functions display some periodicity especially for the cases associated with Locations D–F. The 'period' in terms of time lag, measured peak to peak, can be considered as a rough quantitative estimate of a typical distance between two adjacent data loss clusters/gaps. For example, both the autocorrelation and autocovariance plots (in Figures 9(b) and (c), respectively) for Location F show a dominating periodicity of about 520 time lags (or, DPs). Although the corresponding time history shown in Figure 8 does not exhibit the exact periodicity of the occurrence of data loss, the intervals of those significant data loss clusters (especially between 6000 and 10 000 sample numbers) seem to be fairly consistent with this period based on the autocorrelation and autocovariance functions.

To better comprehend the problem at hand and to illustrate the utility of converting the time histories to a binary signal, the above statistical measures are applied to a series of random binary processes with the same length of 12 000 DPs each. These binary time histories were generated using a set of binomial probability distributions (e.g. [44]) with a probability of a value of 1 at each trial increasing from 0.1 to 0.9 at a step of 0.1. The empirical pdfs, autocorrelation, and autocovariance functions are presented in Plate 1. Shown in the legend is also the actual data loss for each data set. The pdf and autocorrelation plots in Plates 1(a) and (b) clearly demonstrate the effect of the probability of a value of 1 at each trial. The autocovariance plots, however, do not differ greatly from data set to data set. Rather, they all look similar to the one presented in Plate 1(c) when the probability of the value of 1 at each trial is equal to 0.5. Comparing Figure 9 and Plate 1 leads to a quick conclusion that the data loss process studied here is not a Bernoulli-distributed random process. At least, the important independent and identical distribution (i.i.d.) condition is clearly violated as the data loss tends to cluster in time, again, as a result of the adopted flexible payload size scheme shown previously in Figure 4.

### *6.2. Statistical analysis according to testing condition*

For the 9XStream radio (900 MHz) tested at a sampling rate of 500 Hz, all 43 collected time histories (with a non-zero data loss rate) from the results presented previously in Figure 7 are grouped according to their locations (Locations B–F). Each location has a distinct transmitt ing environment and transmitting range associated with it, as shown in Map 2 of Figure 5. For each group, compound histograms of empirical pdfs corresponding to the width of the lost data clusters, average autocorrelation, and autocovariance functions for the first 500 lags are presented in Figures 10(a)–(c), respectively. These results serve as a guideline for the data loss pattern in the specific transmitting environment; however, a large dispersion within each group is observed for the average autocorrelation plots as a result of the widely different data reception



DOI: 10.1002/stc

*Struct. Control Health Monit.* 2008; **15**(4)
DOI: 10.1002/stc

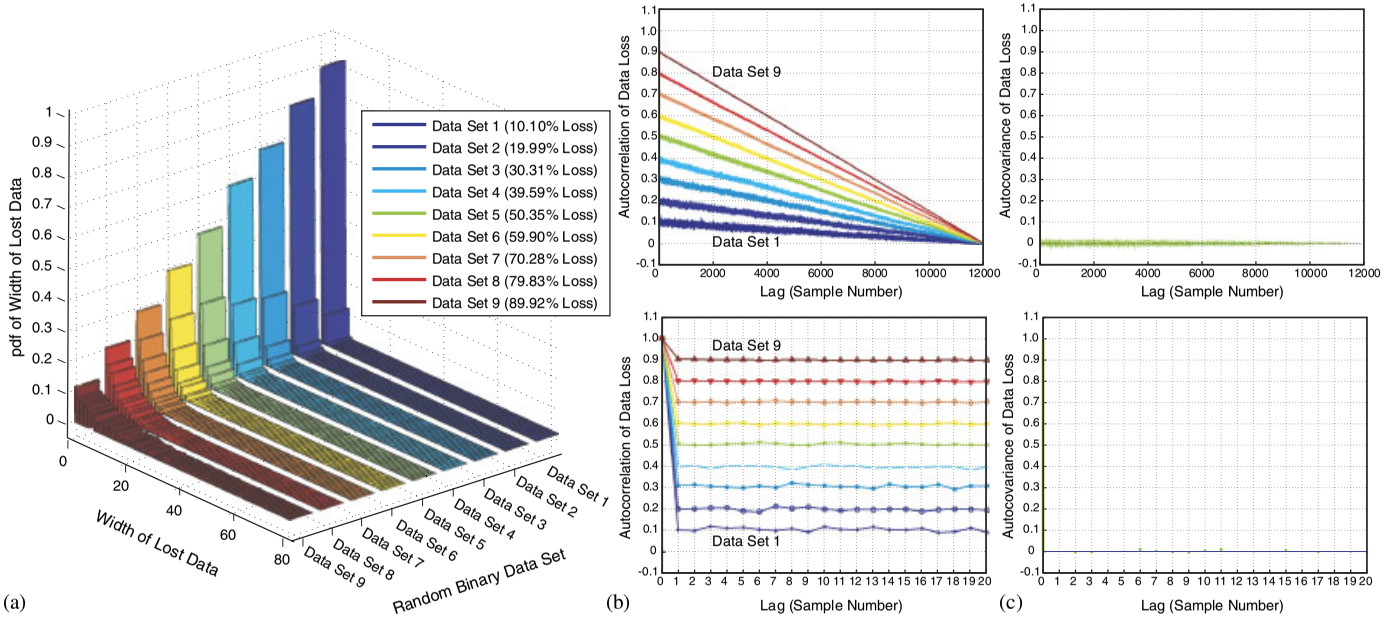


Plate 1. (a) Histograms of empirical probability density functions (pdfs) of the width of lost data; (b) normalized autocorrelation of data loss; and (c) normalized autocovariance of data loss of a set of random binary time histories of 12 000 data points each. These binary time histories were generated using a set of binomial probability distributions [45] with a probability of a value of 1 at each trial increasing from 0.1 to 0.9 at a step of 0.1. The autocovariance plots presented in part (c) are a typical one when the probability of the value of 1 at each trial is equal to 0.5. In both parts (b) and (c), the bottom panels are zoomed versions of the top panels showing only the autocorrelation/autocovariance of the first 20 out of 12 000 time lags.

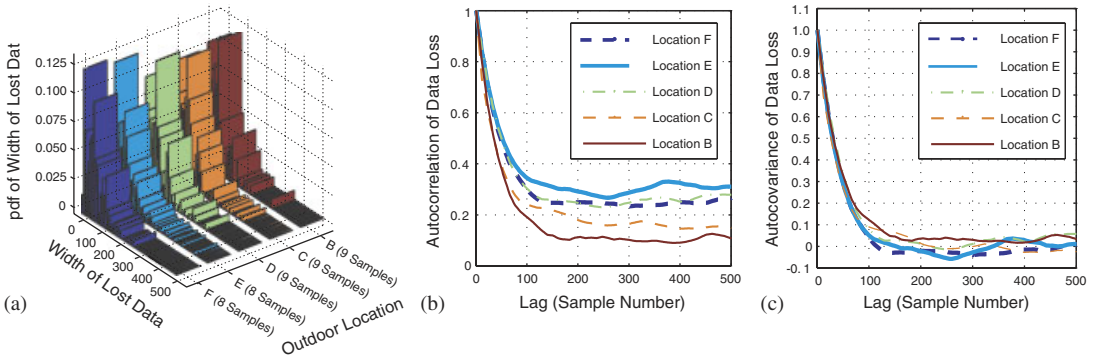


Figure 10. (a) Compound histograms of empirical probability density functions (pdfs) of the width of lost data clusters of all the time histories with a non-zero data loss rate collected using the 9XStream radio (900 MHz) at a sampling rate $f_s = 500$ Hz at the five outdoor (locations B–F shown in Map 2 of Figure 5). (b) Normalized autocorrelation function, and (c) normalized autocovariance function of the data loss of the same time histories. Note that average curves are presented in both (b) and (c).

rates (thus data loss rates) shown earlier in Figure 7. For the 24XStream radio (2.4 GHz), the same exercise is performed on all the time histories collected when having either one router or both routers on. The results also show a large dispersion of the pattern in both groups for the average autocorrelation plot, which again results from a wide range of data loss rate within each group.

### *6.3. Statistical analysis according to data loss rate*

It is further explored if more trackable data loss patterns could possibly be obtained with a relation to data loss rate rather than being guided by the testing configuration as tried above. All the statistical measures suggested in Section 6.1 are applied to all the time histories that are sorted according to their adopted radio, sampling rate, and data loss rate. In detail, all 43 time histories from the 9XStream radio are re-arranged according to their data loss rate (i.e. regardless of their transmitting range). All the time histories collected from the 24XStream radio, mentioned earlier in Section 5.4, are also re-arranged in the same way.

Figure 11 first outlines an overall picture of the effect of data loss rate on the size (including the maximum, minimum, and mean values) and occurrence frequency of lost data clusters by examining all the individual values of data loss rate that ever appeared in this experimental study. Other dominating factors considered are the two types of radios, and two sampling rates used for the 24XStream radios. In addition, the same data loss characteristics of the Bernoulli-distributed random process counterpart are also presented as a comparison (Figure 11(a)). The discrete results for both mean width and occurrence frequency of lost data clusters demonstrate clear trends; fittings are thus applied to them as well as the maximum width of lost data clusters.

While the minimum size of individual lost data clusters is more or less one DP, the maximum size of lost data clusters can vary drastically but with a clear increasing trend with data loss rate. The mean value, however, shows a moderate increasing trend for the X9Stream radio and a nearly constant trend for the X24Stream radio within the range of data loss from 10 to 50%. The occurrence frequency of these lost data clusters nearly linearly increase with data loss rate



DOI: 10.1002/stc

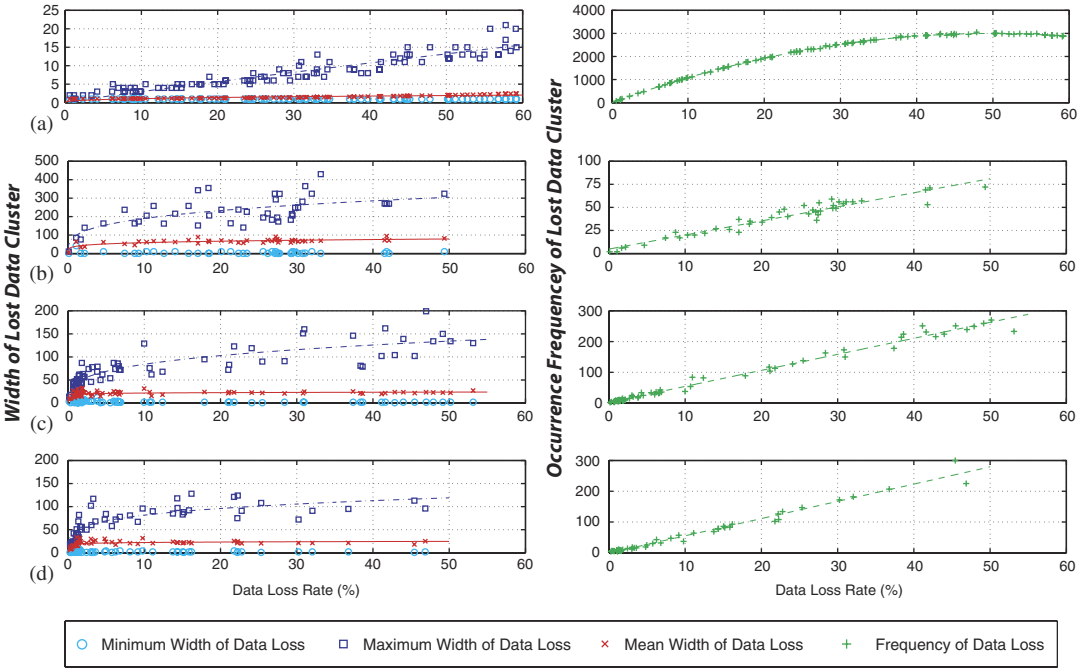


Figure 11. Minimum, maximum, and mean size, and occurrence frequency of the lost data clusters as affected by data loss rate for: (a) 100 simulated binary random time histories; (b) 43 measured time histories using the 9XStream radios (900 MHz) at a sampling rate $f_s = 500$ Hz; (c) 67 measured time histories using the 24XStream radio (2.4 GHz) at a sampling rate $f_s = 500$ Hz; and (d) 49 measured time histories using the 24XStream radio (2.4 GHz) at a sampling rate $f_s = 100$ Hz. The lines are used to fit the discrete points, where the fittings for the maximum and mean size are power functions, and that for the occurrence frequency is either quadratic or linear function.

for both radios. The 100 Bernoulli-distributed random time histories (with 12 000 points each) generated in the way as for Plate 1 shows different trends, which again confirms that the data loss phenomenon studied here is not a simple random binary process. The invariance of the mean width of lost data clusters and the linear increase in the occurrence frequency of the clusters with respect to data loss rate suggests the possibility of simulating such a binary random process as a compound process of the clusters with widths governed by an identical distribution and then spread the clusters out along the time axis using a uniform distribution according to the data loss rate.

Considering the trends established in Figure 11, some insightful observations can be made. Specifically, the average and maximum widths of lost data clusters serve as indicators of the overall quality and reliability of the wireless communication channel. If first the width of lost data clusters is considered, the average width is 69 and 22 DPs for the 9XStream (900 MHz) and 24XStream (2.4 GHz) radios, respectively; this observation is independent of the sampling rate (500 *versus* 100 Hz) and the data loss rate (within the range specified above). The occurrence frequency of lost data clusters plotted as a function of data loss rate provides a quantitative measure of the rate of data loss. As shown in Figure 11(b)–(d), the distribution of occurrence



DOI: 10.1002/stc

frequency *versus* data loss rate follows a linear function whose slope is the rate of the loss. Again, the radios employed is the determining factor with the 9XStream and 24XStream's rates of loss occurring 1.5 and 5 times per percentage of data loss, respectively. The independence of these trends with sampling rate (500 *versus* 100 Hz) is expected.

The data loss rate in all the collected time histories is further divided into five groups, 0–10%, 10–20%, 20–30%, 30–40%, and 40–50%. For each of these five groups, Figure 12 presents a compound pdf of the width of lost data clusters for the two radios at a sampling rate of 500 Hz. It clearly shows distinctly different pdf features for these two radios. Although the trend for the maximum and mean width is consistent with what is observed from Figure 11, the inter-group pattern change is still subtle. This, again, shows the possibility of modelling all the individual lost data clusters to follow an identical distribution, especially for the X24Stream radio.

Figure 13 presents all of the autocovariance plots according to the five groups of data loss rate (0–10, 10–20, 20–30, 30–40, and 40–50%) for the two radios, respectively. The corresponding autocorrelation plots for each reception group are produced; similar patterns as in the autocovariance plot are displayed but with an offset of the values in each plot. This is because the autocorrelation function is clearly affected by the data loss rate while the autocovariance function is not based on their definitions in Equations (2) and (3). Observations made from the autocovariance and autocorrelation plots are as follows:

- Different radios (9XStream *versus* 24XStream) have different autocovariance features. This difference not only exists for the first 500 lags (Figures 13(a) and (b)), but also for the zoomed first 100 lags (Figures 13(c) and (d)). These features can be used to categorize the corresponding time series based upon strong, moderate, or weak autocorrelation, depending on the autoregressive model selected to model each lossy process [44].
- According to the results within the first 100 lag, a strong and moderate autocorrelation category can be assigned to the loss caused by both the 9XStream and 24XStream radios, respectively. The autocovariance plots for the 9XStream radio starts with a very high value at the first lag and then slowly decreases almost linearly with little noise over subsequent lags. Such behaviour suggests that an autoregressive model for the data loss process can be used to predict the data loss. The 24XStream radio displays a smaller value at the first lag and then decreases less linearly with more noise. As a consequence, the predictability of using an autoregressive model for the 24XStream data loss would not be as good as for the 9XStream radio loss process [44]. The nearly linear feature in the 9XStream radio will facilitate a quick adoption of a linear AR model to further simulate the lossy time histories as foreseen earlier in Figure 1 for future simulation effort.
- The periodicity of the peaks in the results for the 24XStream radio can be clearly observed especially when the data loss rate is higher than 30%. A 'period' of about 20 time lags is measured peak to peak from the autocovariance plots. Such a periodicity is expected given an average 'gap' width of 22 DPs (see Figure 11) and a very narrow compound pdf of the width of lost data clusters (see Figure 12). The periodicity in the autocovariance (and autocorrelation) results of the 9XStream is also observed previously in the sample plots in Figure 9(c) (and Figure 9(b)) at Locations D–F. No periodicity can be observed within the first 100 lags for the 9XStreams radio; some ripples can be seen within the first 500 lags. This is because a longer period is expected for the loss from the 9XStreams radio according to the samples in Figures 9(b) and (c), which is likely to be out of the time lag ranges (100 and 500) in this figure. The average 'gap' width for the radio is about 67 DPs



DOI: 10.1002/stc

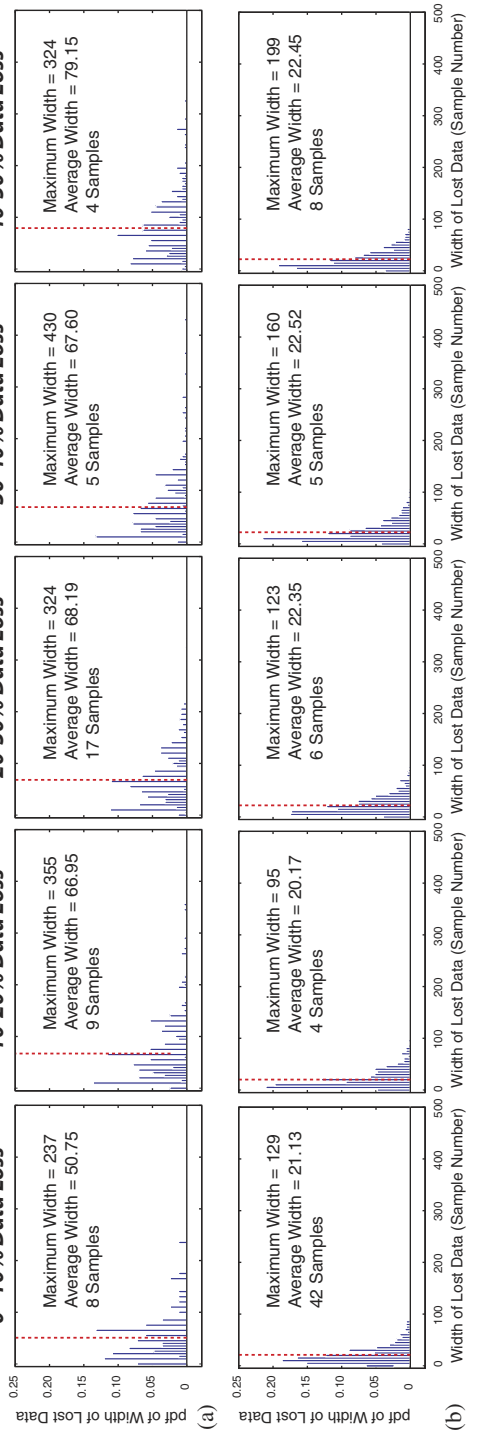


Figure 12. Histograms of empirical probability density functions (pdfs) of the width of data loss using: (a) 9XStream radio (900 MHz) and (b) 24XStream radio (2.4 GHz) according to various ranges of data loss rates. Note the the sampling rate is 500 Hz although it should not affect the pdfs.



DOI: 10.1002/stc

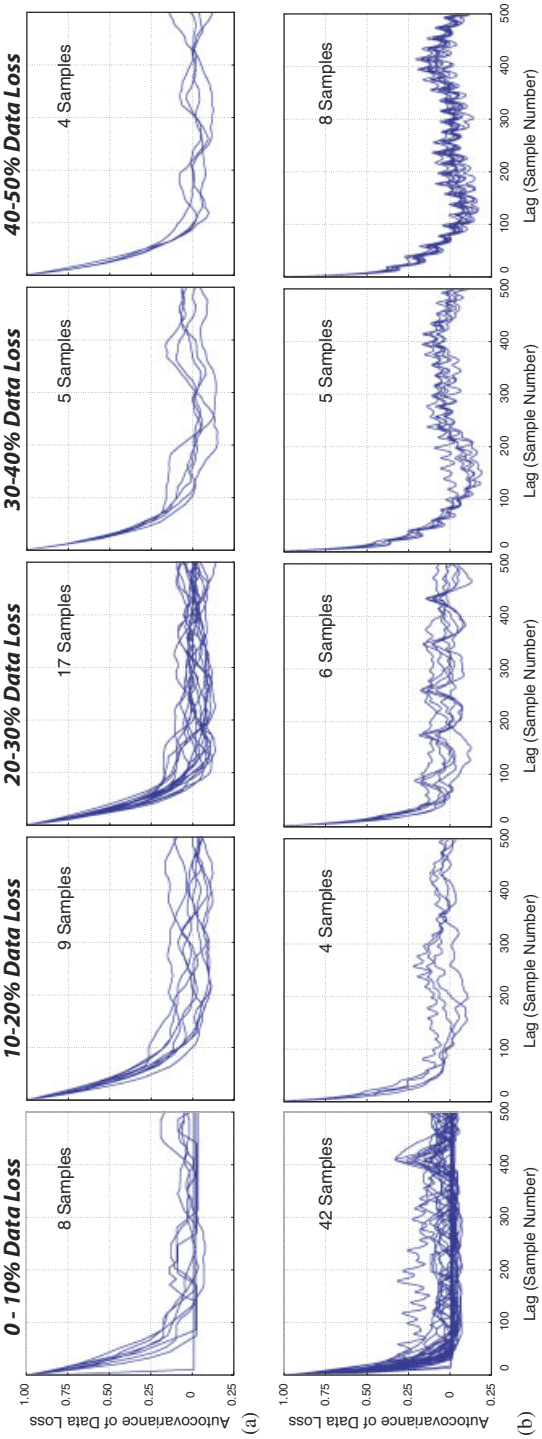


Figure 13. Normalized autocovariance of data loss of the first 500 lags using (a) 9XStream radio (900 MHz) and (b) 24XStream radio (2.4 GHz), both operating at $f_s = 500$ Hz. Normalized autocovariance of data loss of the first 100 lags using (c) 9XStream radio (900 MHz) and (d) 24XStream radio (2.4 GHz), both operating at $f_s = 500$ Hz. Note that the sample number for each plot is indicated on each panel. Part (c) is a zoomed version of part (a), while part (d) is a zoomed version of part (b).



DOI: 10.1002/stc

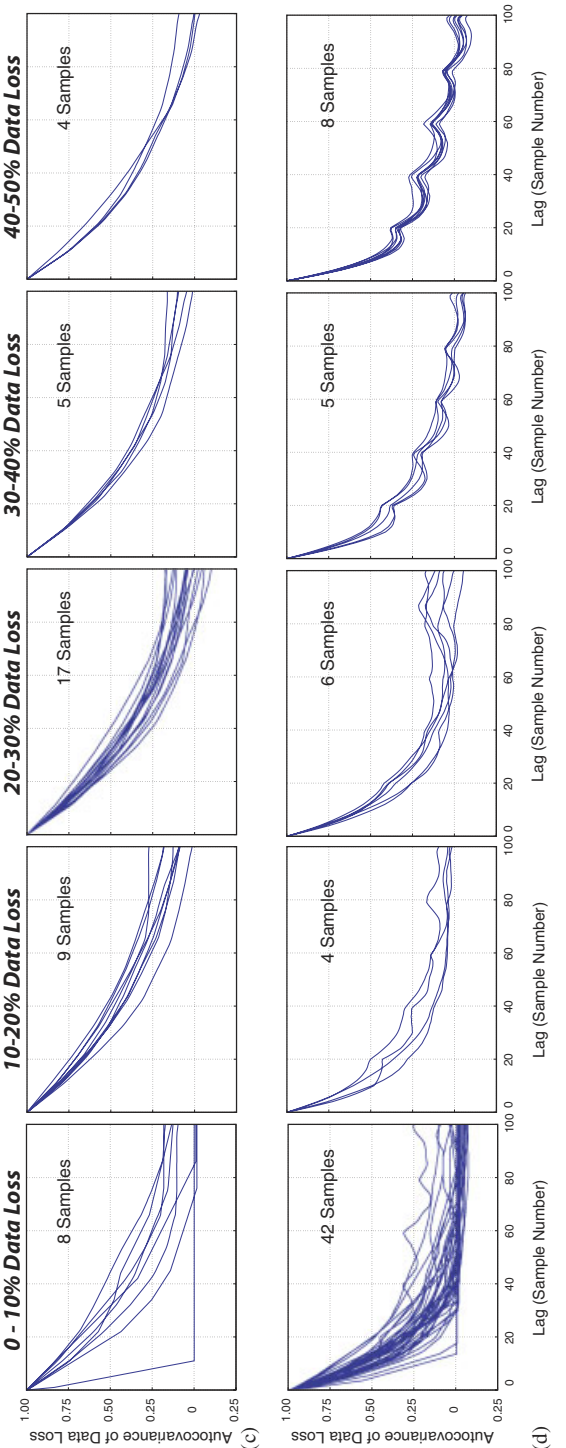


Figure 13. *Continued.*



DOI: 10.1002/stc

(see Figure 11) which is within the smaller time lag range of 100 in this figure; however, the compound pdfs of the width of lost data clusters for the same radio show a feature of multiple peaks (see Figure 12). This complexity makes the loss from the 9XStream radio less periodic than the 24XStream. Recall that there are different carrier frequencies/wavelengths and transmitting powers for the two types of radios. The 24XStream radio is also subjected to inter-channel interference (due to the presence of the 802.11 networking equipment simultaneously operating in the test environment) while the 9XStream radio is not.

- Of the five groups in Figure 13, the plots corresponding to 0–10% data loss rate display the largest variations in the features within the group. It seems that further subdivisions of data loss rate may be needed for this particular group to better extract the underlying loss features. For these cases with low data loss rates, chances to *directly* recover the lost data by properly applying numerical methods are expected to be higher than those cases with higher data loss rates. The statistical features for this particular group as shown in Figures 11 and 13 demonstrate more complicated patterns (e.g. changing average width of lost data clusters), which deserve further studies.

## 7. DISCUSSION

Data loss rather than packet loss is the focus of this wireless communication application-oriented study. It is of critical importance to identify issues related to data quality for the sake of developing robust data processing and system identification tools when using data obtained through wireless sensing. To further demonstrate the significance of investigations along this line, an example of future applications of this work, according to Figure 1, is given as follows by offering recommendations to an end-user of a wireless monitoring system:

1. Perform a series of loopback tests between the locations of potential transmitter and receiver to obtain packet loss rate, based on which a lower bound of data loss rate is estimated (Figure 7).
2. Using this estimated data loss rate, one can then predict the maximum and mean width of the lost data clusters as well as the occurrence frequency (Figure 11).
3. In addition, one can further predict *a priori* other statistical measures of the data loss patterns including histograms of empirical pdf of the width of data loss, and normalized autocovariance of data loss (Figures 12 and 13).
4. Based on this information, one can then design or validate system identification and damage detection algorithms to anticipate and handle these predictable data loss trends.

The severity of data loss and the pattern of loss discovered in this study have clearly revealed the challenge and defined the problem for future work. More work, especially theoretical and analytical work, is required to connect data loss to packet loss so as to make studies like this more beneficial for developing reliable communication protocols for real-time data delivery in a wireless monitoring system. For example, the flexible payload size of the selected MaxStream OEM radios can vary from 1 byte to 64 bytes [35]; how this affects the data loss patterns needs to be investigated.

Attempts have been made throughout this experimental work to consider and then differentiate the effects of various factors contributing to data loss. Loopback tests can be an



DOI: 10.1002/stc

effective option for fast prototyping of the overall effects of all the possible factors. However, more systematic designs of tests are needed to explicitly study the influence of factors such as the operation of rotating machinery and human activities so as to evaluate their effects more quantitatively. In future work, the periodicity in the autocorrelation and autocovariance functions as shown in Figures 9(b) and (c), respectively, needs to be quantified; the stationarity of data delivery performance should also be studied. As a result of these continued efforts, an optimal number of packets used in a loopback test and sampling time used in the transmission of a time history could be derived and further validated by experimental studies.

## 8. CONCLUSION

An experimental study has been carried out to investigate the reliability issue of applying wireless sensing to structural health monitoring. A wireless unit has been developed by using an off-the-shelf microcontroller and radio components; software has been developed to capture the loss of data using a flexible payload scheme when transmitting vibration data from a shake table through various building materials. This study showcases the important attributes of packet (observed from loopback tests) and data (observed from shake table tests) delivery performance of the designed wireless sensing unit. Among all the factors, the attenuation from the building materials, the transmitting range, and transmitting power of the radio dominate the packet delivery performance. For the specific testing environment, the role of foliage attenuation is difficult to differentiate from other factors. For the 24XStream radio, the inter-channel interference from the 802.11b system can be significant and fluctuating as well. It is further experienced in this experimental study that the interference from the operating rotating machinery and human activities can be uncertain under the designed test configuration, necessitating further study.

The phenomenon of data loss has been investigated in terms of data reception rate and loss pattern. The data reception rate is generally consistent with the packet reception rate in a typical loopback test result, which validates the adoption of loopback test as a rapid means for prototyping or characterizing a transmitting environment. The data loss rate is not constant at the same location, which can vary in a range of about 15–35%. The lost DPs tend to cluster in time, which leads to numerical challenges in data processing when no other complex software is used to re-transmit lost DPs especially as required in a near real-time data transmission. The width of these lost data clusters is further measured using pdfs, and it shows an average of 69 and 22 consecutive DPs for 9XStream and 24XStream radios, respectively, at a sampling rate of 500 Hz. These numbers are not generally affected by the sampling rate, and are also found to be insensitive to the experienced data loss rate bounded approximately by 55%. The occurrence frequency of these lost data clusters, however, does strongly depend on the data loss rate. The temporal characteristics of the data loss, as presented in autocorrelation and autocovariance functions, shows a high degree of correlation, which is believed to related to the flexible payload size scheme that is commonly adopted in a wireless transmission channel.

## ACKNOWLEDGEMENTS

This study is primarily supported by the National Science Foundation (SGER CMS-0332350) under Program Officer Dr Steven L. McCabe. The Junior Faculty Research Program awarded to the



DOI: 10.1002/stc

first author by Dr T. H. Lee Williams, the Vice President for Research at the University of Oklahoma, is greatly appreciated. The support from the university program at Analog Devices, Inc. in offering their MEMS accelerometers is gratefully acknowledged. In addition, the assistance offered by Mr Michael F. Schmitz during laboratory testing is deeply appreciated. Some technical assistance offered by Mr Nadim A. Ferzli is appreciated. The participation offered by Miss Anh P. Nguyen at OU in conducting the transmission range tests is acknowledged. Two REU students from Industrial Engineering, Miss Elizabeth Henry from the SUNY Buffalo and Miss Melissa Lindner from the University of Oklahoma, are thanked for their participation and assistance during the preliminary test in summer 2004.

## REFERENCES

1. Donoho L. Wireless develops extrasensory vision of future. *Journal of New England Technology* 2003.
2. Seidel SY, Rappaport TS. 914 mHz path loss prediction model for indoor wireless communication in multifloored buildings. *IEEE Transactions on Antennas and Propagation* 1992; **40**(2):207–217.
3. Wang HS, Moayeri N. Finite state markov channel—a useful model for radio communication channels. *IEEE Transactions on Vehicular Technology* 1995; **44**(1):163–171.
4. Lee KK, Chanson ST. Packet loss probability for real-time wireless communications. *IEEE Transactions on Vehicular Technology* 2002; **51**(6):1569–1575.
5. Tang C, McKinley PK. Modeling multicast packet losses in wireless lans. *Proceedings of the 6th ACM International Workshop on Modeling Analysis and Simulation of Wireless and Mobile Systems*, San Diego, CA. ACM Press: New York, 2003; 130–133.
6. Zhao J, Govindan R. Understanding packet delivery performance in dense wireless sensor networks. *Proceedings of the 1st International Conference on Embedded Networked Sensor Systems*, Los Angles, CA. ACM Press: New York, 2003; 1–13.
7. Shankar PM. *Introduction to Wireless Systems*. Wiley: New York, 2002.
8. Mark JW, Zhuang W. *Wireless Communication and Networking*. Prentice-Hall: Englewood Cliffs, NJ, 2003.
9. Tanenbaum AS. *Computer Networks* (4th edn). Prentice-Hall PTR: Englewood Cliffs, NJ, 2002.
10. Spencer Jr BF, Ruiz-Sandoval ME, Kurata N. Smart sensing technology: opportunities and challenges. *Structural Control and Health Monitoring* 2004; **11**(4):349–368.
11. Clayton EH, Koh B-H, Xing G, Fok C-L, Dyke SJ, Lu C. Damage detection and correlation-based localization using wireless mote sensors. *IEEE International Symposium on Intelligent Control and 13th Mediterranean Conference on Control and Automation*, vol. 1, Limassol, Cyprus, June 2005; 304–309, IEEE Control Systems Society, CSS; Mediterranean Control Association, MCA; Institute of Electrical and Electronics Engineers Inc., Piscataway, NJ 08855-1331, United States.
12. Lynch JP, Loh K. A summary review of wireless sensors and sensor networks for structural health monitoring. *Shock and Vibration Digest* 2006; **38**(2):91–128.
13. Gao Y, Spencer Jr BF, Ruiz-Sandoval ME. Distributed computing strategy for structural health monitoring. *Structural Control and Health Monitoring* 2006; **13**(1):488–507.
14. Chintalapudi K, Paek J, Gnawali O, Fu TS, Dantu K, Caffrey J, Govindan R, Johnson E, Masri S. Structural damage detection and localization using netshm. *Proceedings of the Fifth International Conference on Information Processing in Sensor Networks* (*SPOTS'06*), New York, NY, April 2006; 475–482.
15. Kim S, Pakzad S, Culler DE, Demmel J, Fenves G, Glaser S, Turon M. Health monitoring of civil infrastructures using wireless sensor networks. *Technical Report* UCB/EECS-2006-121, EECS Department, University of California, Berkeley, October 2 2006. http://www.eecs.berkeley.edu/Pubs/TechRpts/2006/EECS-2006-121.html
16. Straser EG, Kiremidjian AS. A modular, wireless damage monitoring system for structures, report no. 128. *Technical Report*, John A. Blume Earthquake Engineering Center, Department of Civil and Environmental Engineering, Stanford University, 1998.
17. Lynch JP, Partridge A, Law KH, Kenny TW, Kiremidjian AS, Carryer E. Design of a piezoresistive mems-based accelerometer for integration with a wireless sensing unit for structural monitoring. *Journal of Aerospace Engineering* (ASCE) 2003; **16**(3):108–114.
18. Lynch JP, Wang Y, Loh K, Yi J, Yun C-B. Performance monitoring of the geumdang bridge using a dense network of high-resolution wireless sensors. *Smart Materials and Structures* 2006; **15**(6):1561–1575.
19. Lynch JP, Sundararajan A, Law KH, Kiremidjian AS, Kenny TW, Carryer E. Embedment of structural monitoring algorithms in a wireless sensing unit. *Structural Engineering and Mechanics*, *Techno Press* 2003; **15**(3): 285–297.
20. Kurata N, Spencer Jr BF, Ruiz-Sandoval M, Miyamoto Y, Sako Y. A study on building risk monitoring using wireless sensor network mica mote. In *Structural Health Monitoring and Intelligent Infrastructure*, Tokyo, Japan,



DOI: 10.1002/stc

13–15 November 2003; 353–357, *Proceedings of the First International Conference on Structural Health Monitoring and Intelligent Infrastructure*, Wu ZS, Abe M (eds). Swets & Zeitlinger B.V.: Lisse, The Netherlands.
21. Ruiz-Sandoval M, Spencer Jr BF, Kurata N. Development of a high sensitivity accelerometer for the mica platform. *Proceedings of the 4th International Workshop on Structural Health Monitoring*, Stanford, CA, 15–17 September 2003; 1027–1034.
22. Glaser SD. Some real-world applications of wireles sensor nodes. *Smart Structures and Materials 2004*: *Sensors and Smart Structures Technologies for Civil*, *Mechanical and Aerospace Systems*, vol. 5391, San Diego, CA, March 2004; 344–355, *Proceedings of SPIE*.
23. Casciati F, Faraveli L, Borghetti F. Wireless links between sensor-device control stations in long span bridges. In *Smart Structures and Materials 2003*: *Smart Systems and Nondestructive Evaluation for Civil Infrastructures*, Liu S-C (ed.), vol. 5057, San Diego, CA, March 2003; 1–7, *Proceedings of SPIE* 2003.
24. Seth S, Lynch JP, Tilbury DM. Wirelessly networked distributed controllers for real-time control of civil structures. *Proceedings of the American Controls Conference* (*ACC2005*), Portland, OR, 8–10 June 2005.
25. Har D, Xia HH, Bertoni HL. Path-loss prediction model for microcells. *IEEE Transactions on Vehicular Technology* 1999; **48**(5):1453–1462.
26. Altman E, Avrachenkov K, Barakat C. A stochastic model of tcp/ip with stationary random losses. *Proceedings of the Conference on Applications*, *Technologies*, *Architectures*, *and Protocols for Computer Communication SIGCOMM '00*, *ACM SIGCOMM Computer Communication Review*, vol. 30. ACM Press: New York, August 2000; 231–242.
27. Tameh EK, Nix AR. The use of measurement data to analyse the performance of rooftop diffraction and foliage loss algorithms in a 3-d integrated urban/rural propagation model. *48th IEEE Vehicular Technology Conference* 1998; 303–307.
28. Kapoor C. Development of reliable and smart wireless sensing units for structural health monitoring. *Master Dissertation*, The University of Oklahoma, Oklahoma, 2005.
29. *12 Bit*, *4 Channel Texas Instrument ADS7841 ADC*. Texas Instruments, http://www.ti.com, a. http://focus.ti.com/lit/ds/symlink/ads7841.pdf
30. *16 Bit*, *4 Channel Texas Instrument ADS8341 ADC*. Texas Instruments, http://www.ti.com, b. http://www.ti.com/lit/ds/symlink/ads8341.pdf
31. *10 Bit*, *4 Channel Texas Instrument TLV1504 ADC*. Texas Instruments, http://www.ti.com, c. http://focus.ti.com/lit/ds/symlink/tlv1504.pdf
32. *CMM-11E1 Single Board Computer*. Axiom Manufacturing, 2004. http://www.axman.com/Pages/neuprod8_cmm11e1.html
33. *XStream-DEV Wireless Development Kits 900 MHz & 2.4 GHz*. MaxStream Inc., 1998–2003. http://www.maxstream.net/products/xstream/devkit/datasheet_XStream_DevKit.pdf
34. *Packetizing Algorithm*. MaxStream Inc., 2004. http://www.maxstream.net/helpdesk/kb.php?kb = 51
35. http://www.maxstream.net/, 2005.
36. Kim Y, Li S. Performance analysis of data packet discarding in atm networks. *IEEE/ACM Transactions on Networking* 1999; **7**(2):216–227.
37. *MaxStream Application Note—Maximizing Range*. MaxStream Inc., 2004. http://www.maxstream.net
38. *ADXL105/ADXL150/ADXL250/ADXL190 Evaluation Modules*. Analog Devices Inc., 2000. http://www.analog.com/UploadedFiles/Evaluation_Boards/Tools/346133416817000 7762ADXL105_190EM_c.pdf
39. *40MS/s Arbitrary Waveform Generator*. National Instruments, 2004. http://www.ni.com/pdf/products/us/3mi469-472.pdf
40. *Portable E Series Multifunction DAQ*. National Instruments, 2004. http://www.ni.com/pdf/products/us/4daqsc205-207_229_238-243.pdf
41. *ConnexLink Development Kits 2.4 GHz*. Aerocomm, Inc, http://www.aerocomm.com. 2005. http://www.aerocomm.com/Docs/Datasheet_ConnexLink.pdf
42. Newland DE. *An Introduction to Random Vibrations*, *Spectral and Wavelet Analysis* (3rd edn). Prentice-Hall: Englewood Cliffs, NJ, 1993.
43. Sólnes J. *Stochastic Processes and Random Vibrations Theory and Practice*. Wiley: New York, 1997.
44. NIST/SEMATECH. *NIST/SEMATECH e-Handbook of Statistical Methods*. National Institute of Standards and Technology, 2005. http://www.itl.nist.gov/div898/handbook/
45. Mendenhall W, Sincich T. *Statistics for Engineering and the Sciences* (4th edn). Prentice-Hall: Englewood Cliffs, NJ, 1994.



DOI: 10.1002/stc